

Lateral variations and vertical structure of the microbial methane cycle in the sediment of Lake Onego (Russia)

Camille Thomas, Victor Frossard, Marie-Elodie Perga, Natacha Tofield-Pasche, Hilmar Hofmann, Nathalie Dubois, Natalia Belkina, Mariya Zobkova, Serge Robert & Emilie Lyautey

To cite this article: Camille Thomas, Victor Frossard, Marie-Elodie Perga, Natacha Tofield-Pasche, Hilmar Hofmann, Nathalie Dubois, Natalia Belkina, Mariya Zobkova, Serge Robert & Emilie Lyautey (2018): Lateral variations and vertical structure of the microbial methane cycle in the sediment of Lake Onego (Russia), *Inland Waters*, DOI: [10.1080/20442041.2018.1500227](https://doi.org/10.1080/20442041.2018.1500227)

To link to this article: <https://doi.org/10.1080/20442041.2018.1500227>



© 2018 The Author(s). Published by Informa UK Limited, trading as Taylor & Francis Group



Published online: 01 Nov 2018.








Submit your article to this journal [↗](#)



View Crossmark data [↗](#)

Lateral variations and vertical structure of the microbial methane cycle in the sediment of Lake Onego (Russia)

Camille Thomas ^{a,*}, Victor Frossard^a, Marie-Elodie Perga^b, Natacha Tofield-Pasche^c, Hilmar Hofmann ^d, Nathalie Dubois ^e, Natalia Belkina ^f, Mariya Zobkova ^f, Serge Robert^g and Emilie Lyautey^a

^aCARTELE, INRA, Université Savoie Mont Blanc, Le Bourget-du-Lac, France; ^bInstitute of Earth Surface Dynamics, University of Lausanne, Lausanne, Switzerland; ^cAPHYS, EPFL, Lausanne, Switzerland; ^dEnvironmental Physics Group, Limnological Institute, University of Konstanz, Germany; ^eDepartment of Surface Waters – Research and Management, Eawag, Swiss Federal Institute of Aquatic Science and Technology, Dübendorf, Switzerland; ^fLaboratory of Paleolimnology, Northern Water Problems Institute, Petrozavodsk, Russia; ^gDepartment of Surface Waters – Research and Management, Eawag, Swiss Federal, Institute of Aquatic Science and Technology, Kastanienbaum, Switzerland

ABSTRACT

The significance of methane production by lakes to the global production of greenhouse gas is well acknowledged while underlying processes sustaining the lacustrine methane budget remain largely unknown. We coupled biogeochemical data to functional and phylogenetic analyses to understand how sedimentary parameters characterize the methane cycle vertically and horizontally in the ice-covered bay of the second largest lake in Europe, Lake Onego, Russia. Our results support a heterogeneous winter methane cycle, with higher production and oxidation closest to riverine inputs. Close to the river mouth, the largest numbers of copies of methane-related functional genes *pmoA* and *mcrA* were associated with a specific functional community, and methane production potential exceeded oxidation, resulting in 6–10 times higher methane fluxes than in the rest of the bay. The elevated fluxes arise from the spatial differences in quantity and type (lacustrine versus riverine sources) of organic matter. More homogeneity is found toward the open lake, where the sediment is vertically structured into 3 zones: a shallow zone of methane oxidation; a transitional zone (5–10 cm) where anaerobic methane oxidation is dominant; and a methane production zone below. This vertical pattern is structured by the redox gradient and human-induced changes in sedimentary inputs to the bay. Retrieved 16S rRNA gene sequences from *Candidatus Methanoperedens* and *Cand. Methyloirabilis* suggest that anaerobic oxidation of methane occurs in these freshwater lake sediments.

ARTICLE HISTORY

Received 30 January 2018
Revised 18 May 2018
Accepted 10 July 2018

KEYWORDS

anaerobic oxidation of methane; lake sediment; *mcrA*; methanogenesis; microbial community

Introduction

Lakes account for 6–16% of the global nonanthropogenic methane (CH₄) emissions (8–48 Tg yr⁻¹), substantially larger than ocean emissions (Bastviken et al. 2004). Continuous reevaluations have now increased this estimate to 76 Tg yr⁻¹ (Saunois et al. 2016), but large uncertainties remain and efforts are ongoing to better constrain CH₄ cycling estimates in time and space (e.g., Brankovits et al. 2017, Davidson et al. 2018). Methane emissions from lake ecosystems are generally the result of the balance between microbial CH₄ production and oxidation. Methane is produced anaerobically in the sediment and in the hypolimnion of stratified lake ecosystems. It is mediated by members of the Archaea domain reducing carbon dioxide (CO₂) using dihydrogen (hydrogenotrophic methanogenesis), acetate (acetoclastic methanogenesis), or sometimes methylated compounds

(methylotrophic methanogenesis) as electron donors. Methane oxidation can occur both aerobically and anaerobically (anaerobic oxidation of methane [AOM]) depending on the availability of electron donors (CH₄) and electron acceptors (e.g., oxygen, sulfate, nitrate; e.g., Borrel et al. 2011). In lakes, AOM is poorly documented despite some indirect indications of its existence. Sulfate-dependent AOM has been suggested in Lakes Cadagno (Switzerland) and Ørn (Denmark) based on isotopic signatures of residual CH₄ and simultaneous concentration measurements and incubations in the sulfate zone (Schubert et al. 2011, Nordi et al. 2013). Incubations in the water column of a meromictic lake in Dendre (Belgium) indicated AOM, in which nitrate instead of sulfate was the electron acceptor (Roland et al. 2016). Sequences related to *Candidatus Methyloirabilis* (formerly NC10), known to perform nitrite-dependent AOM, have been detected in

CONTACT Camille Thomas  camille.thomas@unige.ch

^{*}Current address: Department of Earth Sciences, University of Geneva, Switzerland

© 2018 The Author(s). Published by Informa UK Limited, trading as Taylor & Francis Group

This is an Open Access article distributed under the terms of the Creative Commons Attribution-NonCommercial-NoDerivatives License (<http://creativecommons.org/licenses/by-nc-nd/4.0/>), which permits non-commercial re-use, distribution, and reproduction in any medium, provided the original work is properly cited, and is not altered, transformed, or built upon in any way.

sediments of Lake Biwa in Japan (Kojima et al. 2012) and Lake Constance in Germany (Deutzmann and Schink 2011, Deutzmann et al. 2014). Additionally, it was identified in other freshwater and marine environments reviewed in Welte et al. (2016). Iron (Fe)-supported AOM has also been suggested by biogeochemical measurements in sediments of Lake Ørn in Denmark (Nordi et al. 2013) and Lake Kinneret in Israel (Sivan et al. 2011).

The involvement of sulfate/nitrite/iron reducers in AOM implies that this process is influenced by the production and degradation of intermediate substances used by these consortia, themselves controlled by environmental parameters. In particular, the availability of direct methanogenesis reductants such as acetate or hydrogen (H_2) changes with redox conditions, vertically structuring microbial communities and activities with sediment depth (Conrad et al. 2009). Spatially fluctuating inputs of organic matter or variable sedimentation rates are expected to modify the horizontal structure of communities and activities of the CH_4 cycle (Borrel et al. 2011). We emphasize these vertical and horizontal variations using Petrozavodsk Bay in Lake Onego, Russia, as a study site (Fig. 1).

Elongated, dystrophic Petrozavodsk Bay is fed on one side by the organic matter (OM)-rich Shuya River and opens at its southeast end into the wide oligotrophic Lake Onego, the second largest lake in Europe. The bay thereby creates a contrasting longitudinal gradient with riverine to more lacustrine OM in the sediment. Moreover, anthropogenic activities in its northern watershed in recent decades have markedly influenced the water and sediments of this bay (Kulikova and Syarki 2004, Belkina et al. 2008). As a result, strong changes in the sedimentary column are expected, creating an opportunity to decipher the parameters structuring the

CH_4 cycle in a vertical profile. This knowledge is critical given the current biogeochemical changes and environmental stress applied on lakes and their watersheds by global warming and anthropogenic activities (Palmer et al. 2008, Pachauri et al. 2014). Our objectives were to (1) qualify the actors of this CH_4 cycle, both vertically and along this transect, and (2) identify the structuring parameters influencing the potential variability of this cycle at the bay scale. Our work was conducted during the ice-covered period, which likely constitutes an end member minimum of the carbon cycle in the bay, given lower productivity of lakes during such periods.

To address these objectives, we measured CH_4 pore water concentrations in the sediment and the bottom waters along a transect of the river-influenced Petrozavodsk Bay (Fig. 2, step A). We then quantified CH_4 -related functional genes *mcrA* (involved in methanogenesis; Lueders and Friedrich 2003) and *pmoA* (involved in methanotrophy; Costello and Lidstrom 1999) to distinguish zones of CH_4 production and consumption along depth (Fig. 2, step B). Based on qPCR results, the potential CH_4 production and consumption were measured along the transect to elucidate the functioning of the CH_4 cycle in the Petrozavodsk Bay. We completed the structure of the CH_4 cycle by fingerprinting the *mcrA* functional gene (Fig. 2, step C), which covers both methanogenic and anaerobic CH_4 oxidizing communities (Hallam et al. 2003). Carbon isotopes of pore water CH_4 and sequencing of the *mcrA* and 16S rRNA gene allowed us to further explain the CH_4 related community structure and function with depth (Fig. 2, step D). Accompanying measurements of sediment parameters helped define the vertical structure of the lake sedimentary assemblage as well as the effects of terrestrial inputs on the production and consumption of CH_4 on a horizontal scale.

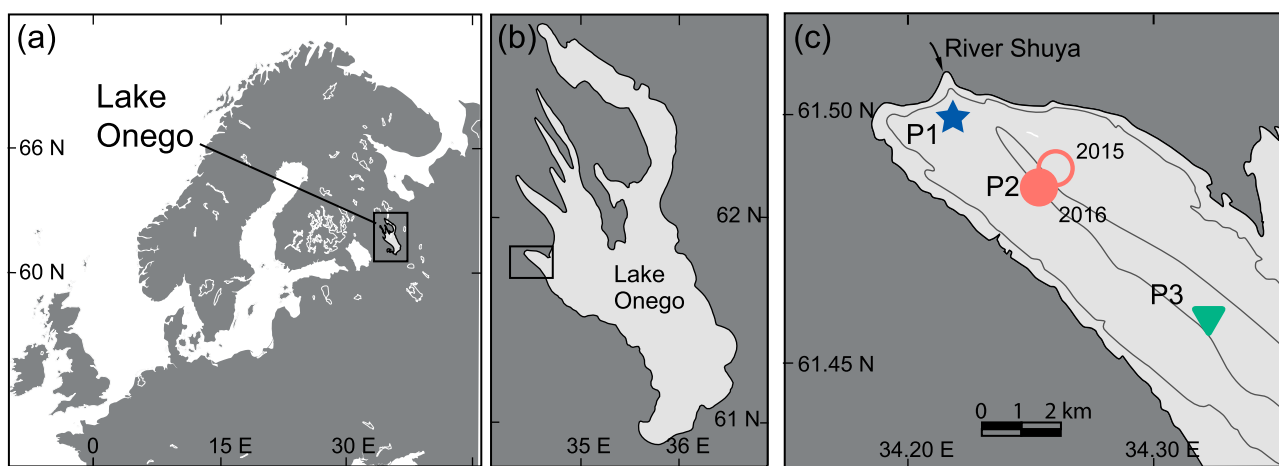


Figure 1. Study site: (a) geographical location of Lake Onego within northern Europe; (b) zoom to Lake Onego area; (c) inset of Petrozavodsk Bay showing the 3 different sites (P1, P2, and P3) along a transect from the Shuya River mouth toward the open lake. Bathymetric lines every 10 m.

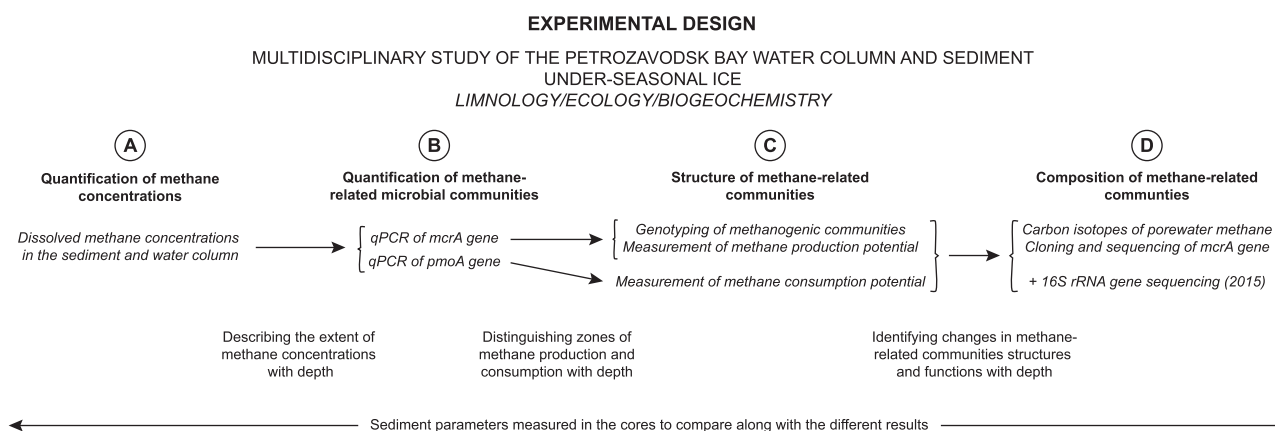


Figure 2. Description of the experimental design and strategy followed to investigate the characteristics of the winter sedimentary methane cycle in Petrozavodsk Bay, Russia.

Limnological setting

Lake Onego, the second largest lake in Europe, has a surface area of 9720 km², an average depth of 30 m, and a maximum depth of 120 m in its northern part. The lake was shaped by successive ice cap advances and retreats that carved relatively deep elongated bays in the northern part of the lake. Petrozavodsk Bay, the main study area, is located in the northwestern part of the lake and owes its name to the city of Petrozavodsk, which flanks its western shore. The bay has a 73 km² surface area and a mean depth of 16 m (Sabylina et al. 2010) and is highly influenced by water from the Shuya River inputs, the second largest tributary of the lake, as well as by runoff from the urbanized area (Sabylina et al. 2010). Runoff has caused eutrophication of the bay during recent decades (Sabylina et al. 2010) compared with the oligotrophic open lake, but the bay remains mesotrophic because of regular water exchange with the main oligotrophic basin. Lake Onego has a low mineralization rate (Belkina 2011), with a notably low contribution of primary production (3%) to the total organic carbon (TOC; Tekanova 2012). Petrozavodsk Bay is often considered dystrophic. Sabylina et al. (2010) estimated that allochthonous OM contributes 61–64% of the total OM in the bay water.

During the ice-covered period (mid-Dec to May), water exchanges between the bay and the open lake vary depending on the extent of the ice cover and seasonal discharge. The bay water can either be highly influenced by the Shuya River or have a similar composition to the open lake. Additionally, little information is available on the quantity of wastewaters discharged to the lake from the city of Petrozavodsk over this period. The water column always remains oxygenated down to the water–sediment interface, even in winter, with oxygen penetrating down into the first 5 cm of sediment (NB, pers. observ.). Despite sporadic winter monitoring,

the physical and biogeochemical functioning of the lake during the ice-covered period is not fully understood, and this poorly studied period is the main focus of a multidisciplinary project from which this study emanates. During the ice-covered period, preliminary results show that, although rates are low, primary production and thermal convection occur in the water column of Petrozavodsk Bay during daytime (Bouffard et al. 2016). Our work is embedded within this joint project and aims to provide insight into the sedimentary CH₄ cycle during the ice-covered period, which likely represents a minimum in the carbon cycling rate compared with the rest of the year.

Material and methods

Sediment coring and on-site sampling

Sediments were collected in March 2015 and 2016 from 3 sites located along a transect extending from the mouth of the Shuya River to the opening of Petrozavodsk Bay (Fig. 1). The 3 sample sites were named as follows from northwest to southeast: P1 (61°49.613'N, 34°22.195'E; 2.2 km from the Shuya River mouth, water depth 10 m); P2 (61°48.744'N, 34°25.793'E in 2015 and 61°48.826'N, 34°25.600'E in 2016; 5 km from the Shuya River mouth, water depth 20 m); and P3 (61°46.707'N, 34°31.797'E; 12.6 km from the Shuya River mouth, water depth 27 m). In 2015, only site P2 was sampled because ice conditions prevented safe access to sites P1 and P3. Sediment cores were retrieved using a gravity corer (Eawag-63/S corer) with 63 mm diameter liners. For each site, 3 cores were collected and dedicated to biogeochemical measurements (CH₄ concentrations and isotopes), microbiological analyses (molecular-based analyses and potential activities), and sedimentological and geochemical analyses. With the exception of the

cores for the sedimentological analyses, the sediment was subsampled on the lake immediately after core retrieval and conditioned according to analysis requirements (after sediment extrusion for potential activities or after sampling through the pierced holes using pre-cut autoclaved syringes for the remaining analyses).

Water and sediment characteristics

Water was sampled using a Niskin bottle at 3 different depths in P1, P2, and P3 in 2016; P2 was also sampled in 2015. The Shuya River sampling site was located at 61° 50.788'N, 34°21.438'E. TOC concentrations were determined using an experimental setup (Zobkov and Zobkova 2015) for the standard UV/peroxodisulphate method (ISO 8245:1999). Data quality control was performed with ICP-Waters project (Escudero-Onate 2016). Color was determined with standard method (ISO 7887:2011), and total Fe concentrations were analyzed by atomic absorption spectrometry. Total organic nitrogen (TON) concentration was determined as the difference between total nitrogen (TN) and the sum of $\text{NH}_4\text{-N} + \text{NO}_3\text{-N} + \text{NO}_2\text{-N}$. TOC, TON, Fe concentrations, and colorimetry in water were analyzed at the Laboratory of Hydrochemistry and Hydrogeology, Northern Water Problems Institute, Karelian Research Center, Russian Academy of Sciences.

The cores dedicated to sediment characterization were transported to the Eidgenössische Technische Hochschule (ETH) laboratory in Zürich, Switzerland, before opening lengthwise. X-ray fluorescence (XRF) was performed on an AVAATECH core scanner (2 mm resolution), and values for elements Fe, titanium (Ti), silicon (Si), calcium (Ca), manganese (Mn), and aluminum (Al) were smoothed over 2 cm and normalized against Al. The working halves of the cores were then sliced at 1 cm resolution for subsequent analyses. Grain size was measured with a Malvern Mastersizer 2000 from Malvern Instruments that measures particle sizes between 0.02 and 2000 μm using laser scattering. XRF core scanning and grain-size analyses were performed at ETH.

Total carbon (TC), total nitrogen (TN), and total sulfur (TS) content was measured on an elemental analyzer (EURO EA 3000), and total inorganic carbon (TIC) was obtained from a titration coulometer (CM5015). TOC was calculated as the difference between total carbon (TC) and TIC. These bulk geochemical analyses were performed at Eawag, Dübendorf, Switzerland.

Methane concentrations, fluxes, and isotope measurements

Sediment samples (2 cm^3) subsampled from the sediment core every centimeter through predrilled holes

were inserted in glass vials with NaOH (4 mL of 2.5% NaOH in 20 mL vials in 2015, and 2 mL of 5M NaOH in 120 mL vials in 2016), covered with a butyl stopper, and sealed with an aluminium crimp. Dissolved CH_4 concentrations were measured in the headspace under controlled temperature conditions and pumped with an automated system (Joint Analytical Systems, Germany) into a gas chromatograph (GC; Agilent) at constant temperature. The GC was equipped with a Carboxen 1010 column (30 m, Supelco) and a flame ionization detector. The oven temperature was 40°C. Methane standards were made by dilution of pure CH_4 (99.9%) and calibrated against commercial references of 100 ppm, 1000 ppm, and 1% (Scott, Supelco).

Methane fluxes (J) were calculated based on Fick's first law using the top 10 cm of measured CH_4 concentrations in 2016 for each site. The equation from Maerki et al. (2004) was used to correct for porosity and tortuosity (Equation 1) with the formation factor F for clay-silt given as $F = 1.02/\varphi^{-1.81}$ and porosity (φ) of 0.9 (same for each site given the similar sediment composition; D. Subetto, pers. comm.). The diffusion coefficient D of CH_4 at 4°C in clay-silt sediment of porosity of 0.9 was $0.67 \times 10^{-5} \text{ cm}^2 \text{ s}^{-1}$ from Iversen and Jorgensen (1993), with J calculated as:

$$J = -\frac{D}{F} \times \frac{\partial \text{CH}_4}{\partial z}. \quad (1)$$

The carbon isotopic signature of CH_4 was determined by a method similar to that described by Sansone et al. (1997). Measurements were taken with an IsoPrime mass spectrometer connected to a TraceGas preconcentrator (GV Instruments, UK). The amount of injected gas depended on the CH_4 concentration in the sample, ranging from a few microliters to several milliliters. Samples were measured twice. Results are noted in the standard δ -notation relative to Vienna PeeDee Belemnite (VPDB):

$$\delta^{13}\text{C}_{\text{CH}_4} = \left(\frac{R_{\text{sample}}}{R_{\text{reference}}} - 1 \right) \times 1000, \quad (2)$$

where R_{sample} is the ratio of $^{13}\text{C}/^{12}\text{C}$ of the sample, $R_{\text{reference}}$ is the ratio of the reference material, and $\delta^{13}\text{C}_{\text{CH}_4}$ is the isotopic signature of CH_4 in ‰ versus VPDB. A standard (1% CH_4 in argon) of known isotopic composition was injected every 2–3 sample runs. The precision of the method was $\pm 0.7\text{‰}$.

The contribution of CH_4 oxidation was estimated based on the difference in $\delta^{13}\text{C}_{\text{CH}_4}$ signatures between 0 and 15 cm. This range was estimated after Bastviken et al. (2002) using equations for an open system in steady state (Equation 3) from Happell et al. (1994) and (Equation 4) from Tyler et al. (1997) and the Rayleigh

model for closed system (Equation 5) from Liptay et al. (1998).

$$f_{open} = \frac{\delta_s - \delta_b}{(\alpha - 1) \times 1000}, \quad (3)$$

$$f_{open} = \frac{\delta_b - \delta_s}{(\delta_s + 1000)((1/\alpha) - 1)}, \quad (4)$$

$$\ln(1 - f_{closed}) = [\ln(\delta_b + 1000) - \ln(\delta_s + 1000)]/(\alpha - 1), \quad (5)$$

where f_{open} and f_{closed} are the fractions of CH_4 oxidized under open and closed system conditions, respectively; δ_s and δ_b are the $\delta^{13}\text{C}_{\text{CH}_4}$ at the surface (0 cm) and bottom (15 cm); and α is the isotope fractionation factor taken as 1.02 (Bastviken et al. 2002). Theoretical $\delta^{13}\text{C}_{\text{CH}_4}$ was also back calculated using the same equations and measured CH_4 oxidation potential (over 24 h).

Sediment potential methane production and oxidation rates

The potentials for CH_4 production and consumption were measured as described in Fuchs et al. (2016) by incubating lake sediment under controlled conditions. Immediately following field sampling, 10 mL of wet sediment per targeted 2–5 cm sections of extruded sediment were placed in 10 mL glass flasks, filled to the top to exclude air capture, sealed, and stored at 4°C until potential activity measurements. Sampled intervals extended to depths of 15 cm at all sites. For CH_4 production potential, 5–10 g of wet sediment was transferred to 150 mL flasks supplemented with 5 mL of demineralized water. The flasks were hermetically sealed with rubber caps, made inert with helium, and incubated at 4°C under constant moderate agitation for 48 h. Methane concentrations were then measured by gas chromatography ($n = 1$) at $t_0 = 1$ h (allowing 1 h of medium equilibration), and at 2, 5, 24, and 48 h using a Catharometer MTI 200 (SRN instruments) equipped with a Poraplot Q 6 m with helium as vector gas. For aerobic CH_4 consumption potential, the same experimental procedure was used, except that 0.3 mL of CH_4 was added to the 150 mL flask headspace through the rubber cap (t_0). The samples were then placed at 4°C under moderate shaking, and CH_4 concentrations were measured after 1, 4, 6, 24, 28, and 48 h using the same device used for CH_4 production. Only the shallowest depth intervals that showed limited CH_4 production (i.e., 0–4 cm for P1, 0–6 cm for P2, and 0–12 cm for P3) were measured for CH_4 consumption potential. For each flask, dry weights of incubated sediments were determined after drying at 105°C for 48 h. Methane production and

consumption were expressed as ng of $\text{CH}_4\text{-C}$ (g^{-1} sediment dry weight [DW] h^{-1}) based on the increase and decrease of CH_4 concentrations, respectively, among $t = 0$, $t = 1$ h, $t = 3$ h ($t = 2$ h for CH_4 consumption), and $t = 24$ h.

Nucleic acids extraction

Core liners were pre-pierced and covered with tape to allow sampling at determined depths (every 1 cm for the first 10 cm and at 15 cm). Samples for nucleic acids-based analyses were taken using pre-cut autoclaved syringes, transferred to cryovials, and immediately stored in liquid nitrogen in the field and at -80°C upon return to the lab (within 10 d) until nucleic acid extraction was carried out. Total DNA was extracted from an average of 1.5 g (0.94–1.89 g) of wet sediment using RNA PowerSoil Total RNA Isolation Kit and RNA PowerSoil DNA Elution Kit (MoBio Laboratories, Carlsbad, CA, USA) according to the manufacturer's protocols. The extracted DNA was quantified fluorometrically after staining with bisBenzimide (DNA Quantitation Kit, Fluorescence Assay, Sigma-Aldrich, St Louis, MO, USA) using a Plate Chameleon fluorometer (Hidex, Turku, Finland; excitation: 340 nm, emission: 460 nm). DNA integrity was verified by automated electrophoresis using the TapeStation 2200 System (Agilent) with the Genomic DNA ScreenTape and Reagents.

High throughput 16S rRNA sequencing and analysis

For this type of analysis, only samples taken in 2015 from site P2 were processed. Polymerase chain reaction (PCR) amplification was carried out with the universal primer 515F (5'-GTGYCAGCMGCCGCGGTA-3') and 909R (5'-CCCCGYCAATTCMTTTRAGT-3') for the V4-V5 hypervariable region of the 16S rRNA gene (Wang and Qian 2009) to which indexes were integrated following the dual-indexing procedure of Kozich et al. (2013). Triplicates of samples were analyzed with ~ 10 ng of DNA per triplicate. Products were then quantified using Picogreen assay (Life Technologies, Carlsbad, NM, USA) and pooled equimolarly. The final pool was purified with AMPure beads after speed-vac concentration. Sequencing was carried out by Fasteris (Geneva, Switzerland) on an Illumina Miseq with 2×250 cycles, with settings of 7.5 Gb yield (including PhiX), an error rate of 2.5%, and Q30 at 75%. The analysis yielded 5.3 Gb of sequences with error rates within quality specifications. Adapters were removed using Trimmomatic (Bolger et al. 2014) by Fasteris. Sequences were then processed using the Find Rapidly

OTUs with Galaxy Solution (FROGS) Galaxy-supported pipeline (Escudié et al. 2018). Paired-end reads were joined using FLASH (Magoč and Salzberg 2011), quality check was performed using FastQC, and contigs were demultiplexed using in-house scripts. Sequences with primers having no mismatch were retained and filtered by size (350–500 bp), and those containing N bases were discarded. The 16S rRNA gene sequences were then denoised and clustered using the Swarm method (Mahé et al. 2015) with a 3-base maximum difference, deleting clusters with <0.005% abundance and cluster occurrence in a minimum of 2 samples of the total library. Chimeras were removed using *vchime* of the *vsearch* package (Rognes et al. 2016). Affiliation was determined using the Silva SSU database 123 (Quast et al. 2013) through BLAST (Altschul et al. 1990), which allowed multiple affiliation and manual curation. Classification at the class level was used for affiliated Bacteria and Archaea. All analyses were performed on the Galaxy instance of the INRA MIGALE bioinformatics platform (<http://migale.jouy.inra.fr>). The relative abundance was calculated against the number of total taxonomically assigned reads, and a constrained hierarchical clustering (UPGMA) using Morisita similarity index and 999 bootstraps was calculated. We present here results from CH₄-related Archaea and Bacteria evaluated at the order/family level. These sequences are available at GenBank under the accession numbers MH205692 to MH205728.

Microbial community abundances

The abundance of methanogens and methanotrophs was estimated by quantitative PCR of *mcrA* and *pmoA* genes for the 3 sites in 2016. Results from P2 (2015) were also added for comparison. The protocol used was the same as described by Fuchs et al. (2016) with a final qPCR mix adjusted to 25 µL. Reactions were performed in a final volume of 25 µL, containing 1× Brilliant II SYBR Green QPCR Master Mix (Agilent), 0.3 mg mL⁻¹ of bovine serum albumin (Sigma-Aldrich), 0.5 µM of each primer, and 0.5 µL of DNA. A plasmid containing a single copy of *mcrA* and *pmoA* genes amplified from a *Methanosarcina thermophila* affiliated clone (KR011363) and from *Methylomonas methanica* DSMZ 25384 DNA extract, respectively, was diluted from 10⁷ to 10¹ molecules per assay. Samples and standards were used in triplicate. Efficiencies were 93% for *mcrA* and 99% for *pmoA*. Relative standard deviations were calculated with a 10% allowed maximum. An ANOSIM test was computed to compare sites on PAST (Hammer et al. 2001), using a Bray-Curtis similarity matrix with 9999 permutations.

Fingerprinting of functional gene *mcrA*

Extracted DNA was amplified using primers ME1 (5'-6-FAM-labelled-) and ME2 as described by Billard et al. (2015) but with modified hybridization temperature to 54°C. Amplicons were then digested using the *MspI* restriction enzyme for 4 h at 37°C. Restriction products were purified using a AxyPrep PCR Clean-up Kit (Axygen, Tewksbury, MA, USA) and separated on an ABI 3730xl DNA Analyzer (BIOfidal DTAMB, Université Lyon 1) using the internal size standard Dye 5 ladder, 50–1000 bp (Gel company, San Francisco, CA, USA). Fragments were then treated using the PeakScanner software, with a fluorescence cutoff of 15 relative fluorescence units, and then processed with the interactive biner method (Ramette 2009) using WS = 2, Sh = 1, and cutoff of 0.01.

The obtained distance values for each operational taxonomic unit (OTU) were exponentially transformed ($c = 2$) and plotted by principal coordinates analysis (PCoA) using a Bray-Curtis similarity calculation. We computed an analysis of similarities (ANOSIM) on PAST (Hammer et al. 2001) using a Bray-Curtis similarity matrix and 9999 permutations for testing the difference between user-defined groups. A Bonferroni correction was applied to assess significance, which was always below $p = 0.0002$ with $R = 0.33$. A Venn diagram was constructed using *Mothur* (Schloss et al. 2009).

Cloning and sequencing of functional gene *mcrA*

Samples were selected based on significant clusters obtained from T-RFLP to construct 4 clone libraries. Amplicons of *mcrA* of samples P2 (5 cm) and P3 (8 cm) were cloned individually. Samples from 2 and 4 cm from site P1 were pooled and named P1, and a pool containing a few rare OTUs (including 3 samples: P2 [2 cm] from 2015, P1 [10 cm], and P2 [1 cm]) was named PP. Amplicons were cloned into pGEM-TEasy TA vector (Promega) according to the manufacturer's protocol with an insert/vector ratio adjusted to 1 for each reaction. For each library, 96 clones were sent to MacroGen Europe (Netherlands) for purification and sequencing using T7 primer. Obtained sequences were aligned using clustalW on MEGA (Kumar et al. 2016), checked for chimeras manually and with Uchime (Edgar et al. 2011), and classified in 95% similar OTUs (Daebeler et al. 2013) on *Mothur* (Schloss et al. 2009). BLAST was conducted with *blastn* from the National Center of Biotechnology Institute database (Johnson et al. 2008), and the resulting sequences were aligned by amino acids and used to build a phylogenetic tree using the neighbor-joining method (Saitou and Nei

1987) with 1000 samples bootstrapped on MEGA (Kumar et al. 2016). Sequences are available in the NCBI database under the accession numbers MG594064 to MG594136.

Cloning results were correlated to T-RFLP fragments by performing *in silico* T-RFLP on the *mcrA* sequences using TRiFLe (Junier et al. 2008). Simulated fragments that varied from experimental fragment size by <3 bp were considered. These results were used to complete sequence occurrence for each site. Weighted phylogenetic distance (Unifrac) was calculated for P1, P2, and P3 based on the obtained final tree using *Mothur* (Schloss et al. 2009).

Data analysis

Data obtained from XRF-scanning were presented as profiles with depth points 2, 4, 6, 8, 10, and 15 cm, selected after smoothing over 2 cm. These points were plotted against Al for easier representation. Percent sand, TOC, C/N, and TS were selected for the same sediment depths. When data were missing for the corresponding depth, the average between 2 intermediate depths was considered.

We built 2 community matrixes: the first was an OTU versus sites matrix based on *mcrA* TRFLP results (relative fluorescence), and the second was an OTU versus sites matrix based on selected 16S rRNA gene abundance of methanotrophic microbial clades. Environmental parameters fitting the matrix samples' depths were compiled in an associated variable table. The functional and microbial dataset were both range-transformed. We then computed several distance-based redundancy analyses (dbRDA) as an ANOVA to test for the possible influence of environmental variables in driving the communities. First we tested whether depths and sites were significant variables influencing the structure of these

communities. We then tested the significance of sedimentary parameters in structuring these communities. The parameters were standardized and their significance was assessed using automatic stepwise (forward) model building for constrained ordination with 5000 permutations. All analyses were performed using the *Vegan* package (Oksanen et al. 2007) and R 3.4.0 (R Core Team 2015).

Results

Water and sediment characteristics for each site

The Shuya River entering at the head of the bay significantly affects the hydrochemical regime of the entire bay. TOC, TON, and Fe concentrations and color were maximal in the river at 18.0, 0.87, and 1.23 mg L⁻¹, and 138 mg Pt L⁻¹, respectively, in March 2016. TOC concentration decreased from head to edge of the bay (Table 1), but maxima were measured in P2 at 12 m (17.3 mg L⁻¹). Minimum values were measured for each site at the deepest sampling points. Overall, the C/N ratio was exceptionally high for each site (>30) at the shallowest and intermediate depths and was lowest at the deepest depths, with 26.7, 23.3, and 15.6 for P1, P2, and P3, respectively. The color indices showed maximum turbidity for the Shuya River decreased with distance from the river mouth. Color index and TOC concentrations at P2 station were close to values in the open lake water in March 2015 and close to values in the river water during the same period in 2016 (Table 1).

Profiles of the environmental variables exhibited different patterns in the first 15 cm (Fig. 3a). Al, Si, Ca, Ti, and Fe all behaved similarly, but quantitative differences were clearly observed for Fe/Mn and C/N for P1 as well as the depth occurrences of peak values (e.g., percent sand and TS). Alkalinity was so low it was not

Table 1. Water column total organic carbon, total nitrogen, iron contents, C/N molecular ratio, and colorimetric index at various depths for sites P1, P2 (2016 and 2015), and P3, as well as for the Shuya River.

Station	Season	Depth m	TOC mg L ⁻¹	TON mg L ⁻¹	TN mg L ⁻¹	Fe mg L ⁻¹	Color mg Pt L ⁻¹	C/N (atomic ratio)
River Shuya	March 2016	0.5	18	0.87	1.04	1.23	138	20.2
P1	March 2016	1	15.7	0.31	0.47	0.74	116	39.0
		10	16.6	0.36	0.47	0.76	117	41.2
		21	8.7	0.2	0.38	0.18	45	26.7
		1	13.4	0.26	0.42	0.51	89	37.2
P2	March 2016	12	17.3	0.38	0.48	0.93	132	42.0
		24	7.6	0.35	0.38	0.10	32	23.3
		1	12.2	0.25	0.4	0.42	83	35.6
P3	March 2016	15	9.8	0.19	0.37	0.25	63	30.9
		30	7.6	0.22	0.57	0.14	35	15.6
		0.5	7.3	—	—	0.15	33	—
P2	March 2015	4	8.4	—	—	0.15	33	—
		10	8.3	—	—	0.15	33	—
		18	8.2	—	—	0.15	34	—
		24	7.2	—	—	0.16	33	—
		26	7.2	—	—	0.16	34	—
		26	7.2	—	—	0.16	34	—

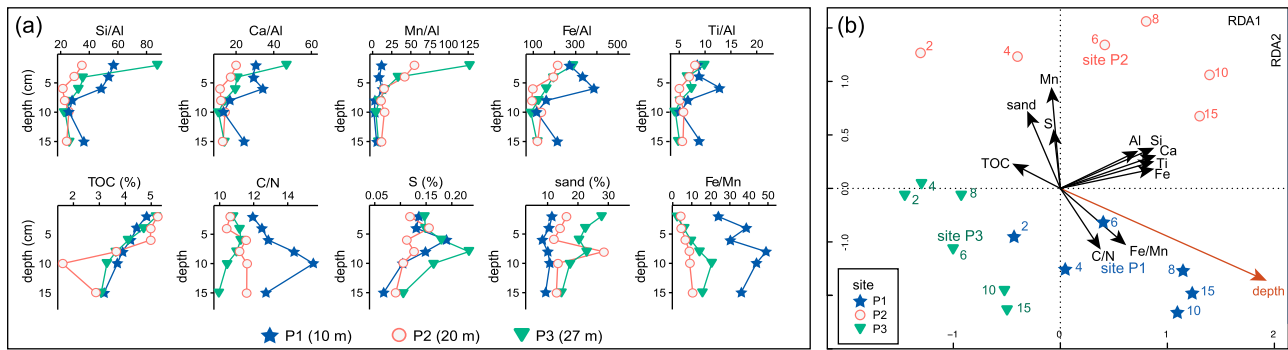


Figure 3. Vertical profiles of (a) environmental parameters and (b) redundancy analysis of measured sediment cores at the sites P1 (2016), P2 (2015), and P3 (2016) in Petrozavodsk Bay. X-ray fluorescence (XRF) data are plotted against aluminum (Al) to allow inter-site comparison. Color-coding in all figures is as follows: P1 = blue stars, P2 (2015) = open red circles, and P3 = green triangles.

plotted. An RDA highlighted inter-site environmental differences (Fig. 3b) and indicated the structuring effect of depth in the environmental profile ($p = 0.001$).

Methane concentrations, fluxes, and stable isotope composition

Methane concentrations and stable isotopes composition were measured for the first 15 cm of the sediment core only because we expected this range would reveal the

main variations in the CH_4 cycle, as is generally the case in large lakes. At all 3 sites, the CH_4 profiles exhibited similar diffusive behavior but with increasing gradients from P3 to P1 (Fig. 4a). The highest pore water CH_4 concentrations occurred at the lowest end of the analyzed vertical range, with a maximum $>1704 \mu\text{mol L}^{-1}$ at 14 cm for P1, $288 \mu\text{mol L}^{-1}$ at 14 cm for P2, and $101 \mu\text{mol L}^{-1}$ at 10 cm for P3. At site P2 in 2015, a similar profile was recorded with concentrations increasing up to $512 \mu\text{mol L}^{-1}$ at 40 cm. In the first centimeter of the sediment, CH_4

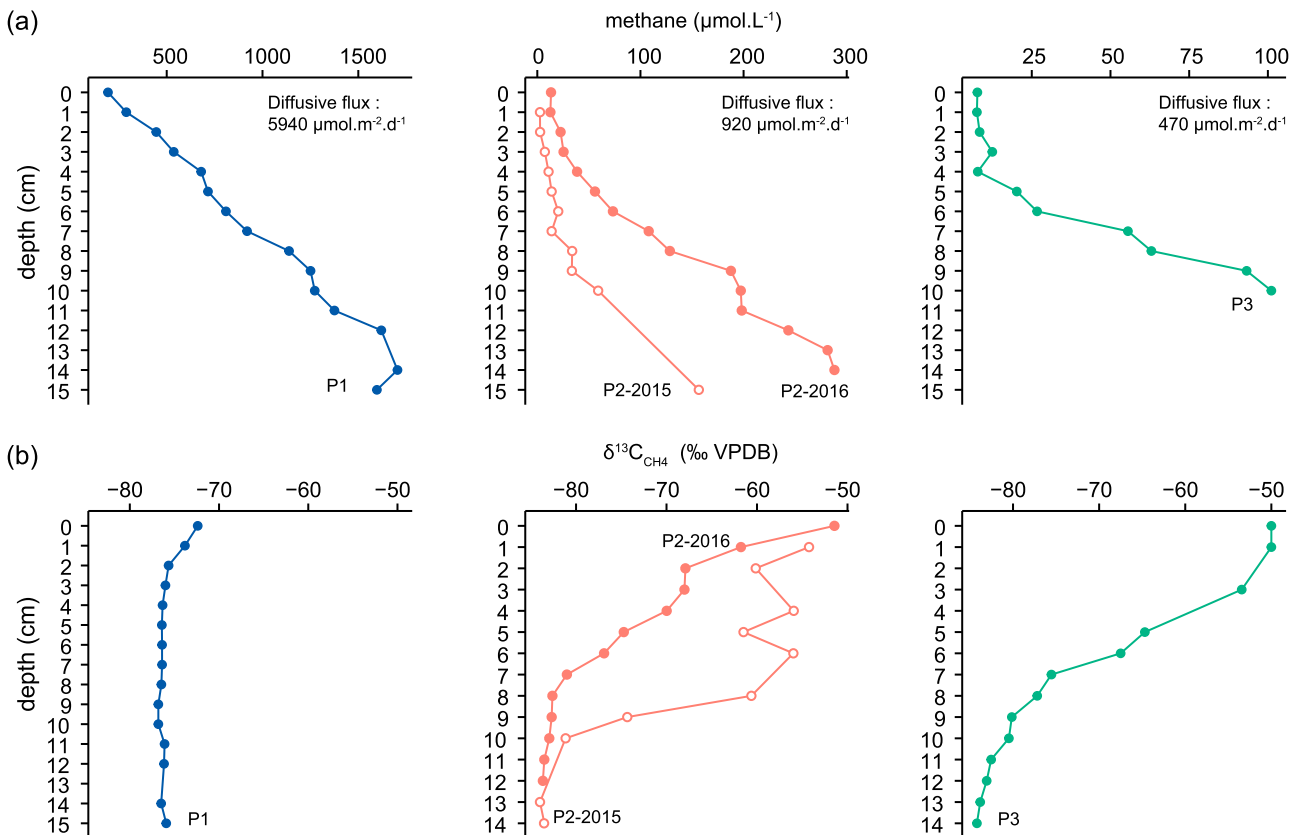


Figure 4. Sedimentary profiles of (a) methane concentrations and (b) ratio of carbon isotopes from methane in Petrozavodsk Bay. Calculated methane diffusive fluxes are given for the 2016 measurements.

concentrations were highest at site P1 (193 $\mu\text{mol L}^{-1}$) compared to 4.9, 13.3, and 7.7 $\mu\text{mol L}^{-1}$ at sites P2 (2015), P2 (2016), and P3, respectively. Fluxes were estimated at 5.94 $\text{mmol m}^{-2} \text{d}^{-1}$ for P1, 6.5 times more than the 0.92 $\text{mmol m}^{-2} \text{d}^{-1}$ calculated for P2 (Fig. 4a). The CH_4 flux at P3 was 0.47 $\text{mmol m}^{-2} \text{d}^{-1}$, half of that measured in P2. Methane concentrations in the bottom waters were below detection limits for all sites except for P3, where they reached 21 nmol L^{-1} .

At P1, stable isotopic ratios of CH_4 carbon were relatively stable around -76.4‰ (SD 0.3‰) and increased in the upper 2 cm toward the sediment–water interface to -72.4‰ (Fig. 4b). At P1, $\delta^{13}\text{C}_{\text{CH}_4}$ in the upper 5 cm was lighter than at site P2(2015) and P2(2016) as well as at P3. For P2, values in the upper 8 cm differed between 2015 and 2016. In 2015, $\delta^{13}\text{C}_{\text{CH}_4}$ values averaged -57.6‰ in the upper 8 cm and -82.4‰ below 10 cm. The difference between the 2 years may be related to the spatial heterogeneity of the sediment because cores were not taken in exactly the same location each year, or because the water chemistry changed between 2015 and 2016 (Table 1). A transition was observed at 10 cm with an intermediate $\delta^{13}\text{C}_{\text{CH}_4}$ value of -74.3‰ . In 2016, minima around -83‰ were observed between 7 and 15 cm, and then values increased regularly until 2 cm to -68‰ and finally reached -51.4‰ at the sediment–water interface. For P3, minimum values lower than -80‰ were measured below 9 cm, increased rapidly from -75.5‰ to -53.4‰ between 7 and 3 cm, and reached approximately constant, maximum values of about -50‰ for the most superficial sediments.

Calculations in open and closed systems showed that only $\sim 20\%$ of the CH_4 was oxidized in P1 in the top 15 cm of sediment, which is substantially lower than that observed in P2 and P3 (81.6 and 83.8% in closed

systems, respectively), and $>100\%$ in the open system (Table 2a). Calculations of theoretical $\delta^{13}\text{C}_{\text{CH}_4}$ gave values relatively heavier than those measured in P1 (-71.7‰ and -69.3‰ in a closed system, compared to -76.4‰ to -72.4‰ measured between 4 cm and 0 cm). For P2 and P3, the calculated $\delta^{13}\text{C}_{\text{CH}_4}$ values were generally lower than the measured values, in particular in the shallowest regions, and reached a maximum of -75.9‰ in the most surficial intervals regardless of the system. Such signatures were already exceeded at 5 and 6 cm for P2 and P3 and gave $\delta^{13}\text{C}_{\text{CH}_4}$ values of -51.4‰ and -50‰ , respectively, near the sediment–water interface.

Methane production and consumption potential

Potential CH_4 production rates exhibited different magnitudes according to the site or sediment layer considered. At P1, a $\text{CH}_4\text{-C}$ (DW) production peak reaching 185 and 213 $\text{ng of CH}_4\text{-C g}^{-1} \text{h}^{-1}$ (over 24 h) between 6–8 cm and 4–6 cm, respectively, was observed (Table 3a). By contrast, lowest production with $<50 \text{ ng CH}_4\text{-C g}^{-1} \text{h}^{-1}$ occurred in the upper 4 cm and between 10 and 15 cm (24 h). At P2, CH_4 production potential reached a maximum of 18 $\text{ng CH}_4\text{-C g}^{-1} \text{h}^{-1}$ between 8 and 10 cm (24 h). It stabilized at 16 $\text{ng CH}_4\text{-C g}^{-1} \text{h}^{-1}$ between 6 and 8 cm

Table 3. Measured potential (a) methane production and (b) consumption rates at sites P1, P2, and P3 in 2016 during the first hour, the first 3 h (the first 2 h, for consumption) and the first 24 h.

(a) Methane production ($\text{ng C-CH}_4 \text{ g}^{-1} \text{ DW h}^{-1}$)				
site	depth	over 1 h	over 3 h	over 24 h
P1	0–2 cm	0	0	11
	2–4 cm	69	109	48
	4–6 cm	289	456	213
	6–8 cm	309	27	185
	8–10 cm	130	203	100
	10–15 cm	15	23	10
P2	0–2 cm	0	0	0
	2–4 cm	54	65	12
	4–6 cm	25	29	8
	6–8 cm	49	59	16
	8–10 cm	54	65	18
	10–15 cm	22	26	5
P3	0–3 cm	0	0	0
	3–6 cm	0	0	0
	6–9 cm	0	0	0
	9–12 cm	6	8	0
	12–15 cm	36	43	8
(b) Methane consumption ($\text{ng C-CH}_4 \text{ g}^{-1} \text{ DW h}^{-1}$)				
site	depth	over 1 h	over 3 h	over 24 h
P1	0–2 cm	–34 502	–18 057	–1346
	2–4 cm	–34 158	–18 803	–1425
P2	0–2 cm	–19 594	–10 945	–841
	2–4 cm	–17 370	–9771	–757
	4–6 cm	–15 719	–8962	–706
P3	0–3 cm	–25 230	–14 573	–1163
	3–6 cm	–13 652	–7983	–647
	6–9 cm	–20 058	–11 799	–963
	9–12 cm	–12 204	–7262	–601

(a) Theoretical fraction (%) of oxidized methane based on measured δs and δb			
	Equation 3	Equation 4	Equation 5
P1	20.0	22.0	19.4
P2	158.0	169.9	81.6
P3	170.0	182.5	83.8

(b) Theoretical δs (‰) calculated from methane oxidation potentials			
P1 0–2 cm	–67.3	–68.7	–69.3
P1 2–4 cm	–70.9	–71.3	–71.7
P2 0–2 cm	–75.9	–76.6	–77.2
P2 2–4 cm	–78.3	–78.5	–78.9
P2 4–6 cm	–80.0	–80.0	–80.3
P3 0–3 cm	–76.1	–77.0	–77.7
P3 3–6 cm	–79.0	–79.3	–79.7
P3 6–9 cm	–80.8	–80.8	–81.1
P3 9–12 cm	–81.0	–81.0	–81.3

but reached ~ 50 ng CH₄-C g⁻¹ h⁻¹ between 6 and 10 cm (and at 2–4 cm) in the first hours of incubation. At P3, the CH₄ production zone was deeper compared to the other sites, starting only at 12 cm (8 ng CH₄-C g⁻¹ h⁻¹ over 24 h, and 36 ng CH₄-C g⁻¹ h⁻¹ in the first hour).

The potential consumption of CH₄ was also higher at P1 (Table 3b). The maximum CH₄ consumption of about 1425 ng CH₄-C g⁻¹ h⁻¹ was measured between 2 and 4 cm (over 24 h) and about 1346 ng CH₄-C g⁻¹ h⁻¹ between 0 and 2 cm. It reached 34 502 ng CH₄-C g⁻¹ h⁻¹ in the first hour between 0 and 2 cm (34 158 ng CH₄-C g⁻¹ h⁻¹ between 2 and 4 cm). At P2, maximal consumption rates of 841 ng CH₄-C g⁻¹ h⁻¹ (over 24 h) and 19 594 ng CH₄-C g⁻¹ h⁻¹ were measured between 0–2 cm over the first hour. Values dropped to 757 and 706 ng CH₄-C g⁻¹ h⁻¹ over 24 h between 2–4 cm and 4–6 cm, respectively. At P3, CH₄ consumption was higher than at P2, with 1163 ng CH₄-C g⁻¹ h⁻¹ between 0 and 3 cm (25 230 ng CH₄-C g⁻¹ h⁻¹ over the first hour) and 963 ng CH₄-C g⁻¹ h⁻¹ between 6 and 9 cm (20 058 ng CH₄-C g⁻¹ h⁻¹ over the first hour). Values dropped to 647 and 601 ng CH₄-C g⁻¹ h⁻¹ (over 24 h) between 3 and 6 cm and 10 and 15 cm, respectively. However, rates for P1 are possibly overestimated while those of P2 and P3 may be underestimated. Calculations of $\delta^{13}\text{C}_{\text{CH}_4}$ for site P1 were heavier, suggesting that the maximum CH₄ oxidation potential is not attained *in situ*. We suggest this result was caused by the low oxygen penetration in this site, which prevented the establishment of aerobic methanotrophy, unlike in incubation experiments that occurred in oxidizing conditions. By comparison, sites P2 and P3 with theoretical $\delta^{13}\text{C}_{\text{CH}_4}$ values are much higher than actually

observed (0–6 cm). We interpreted this finding as the effect of AOM, which was not taken into account in the incubation method.

Functional gene quantification, structure, and drivers

The number of *mcrA* copies varied for each site, with a maximum of 1.4×10^7 copies g⁻¹ DW at P1 (7 cm), 1.2×10^7 at P2 in 2015 (10 cm), and 5.9×10^4 (20 cm) in 2016 (Fig. 5a). Site P3 overall exhibited the lowest values, never exceeding 4.7×10^3 copies g⁻¹ DW at 2 cm depth. At P1, strong variations were observed between maximum and minimum values in the first 10 cm. Copy number dropped below 10^3 g⁻¹ DW under 10 cm. At P2, the number of *mcrA* copies was much higher in 2015 than in 2016 (by 2 to 4 orders of magnitude). Although the magnitude in *mcrA* copies at P2 varied between years, the vertical structure of both was similar, with an increasing trend in the upper 10 cm. Significant differences were observed between P1 and the other sites (Bonferroni-corrected *p* value of 0.08 between P1 and P2, and 0.006 between P1 and P3).

In general, at all 3 sites the maximum *pmoA* copy number was highest, with about 10^5 copies g⁻¹ DW in the upper 7 cm, and decreased at greater sediment depths to about 10^3 copies g⁻¹ DW (Fig. 5b). The maximum *pmoA* copy number was observed at 7 cm at P1 with 3.3×10^5 copies g⁻¹ DW and stayed above 10^5 copies g⁻¹ DW in the first 7 cm. At P2, a maximum of $>10^5$ copies g⁻¹ of sediment was observed in the upper 7 cm in both years. At site P3, the maximum *pmoA* copy number reached 2.4×10^5 g⁻¹ only at 5 cm and dropped to 5.0×10^3 copies at 15 cm.

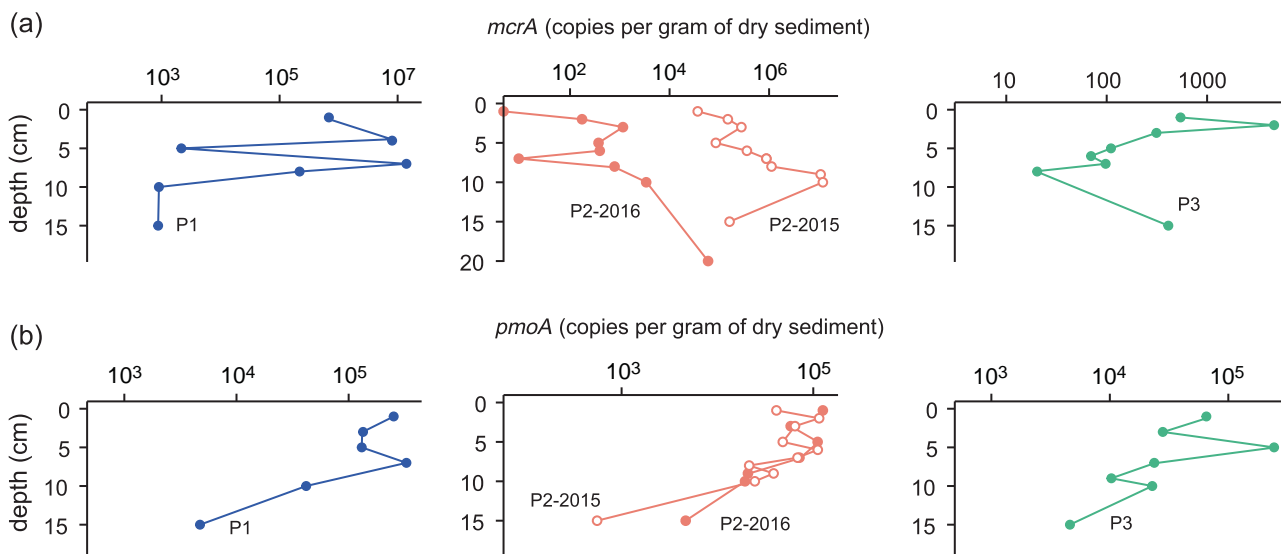


Figure 5. Number of (a) *mcrA* and (b) *pmoA* gene copy numbers for the 3 Petrozavodsk Bay sites P1, P2, and P3 along the cores.

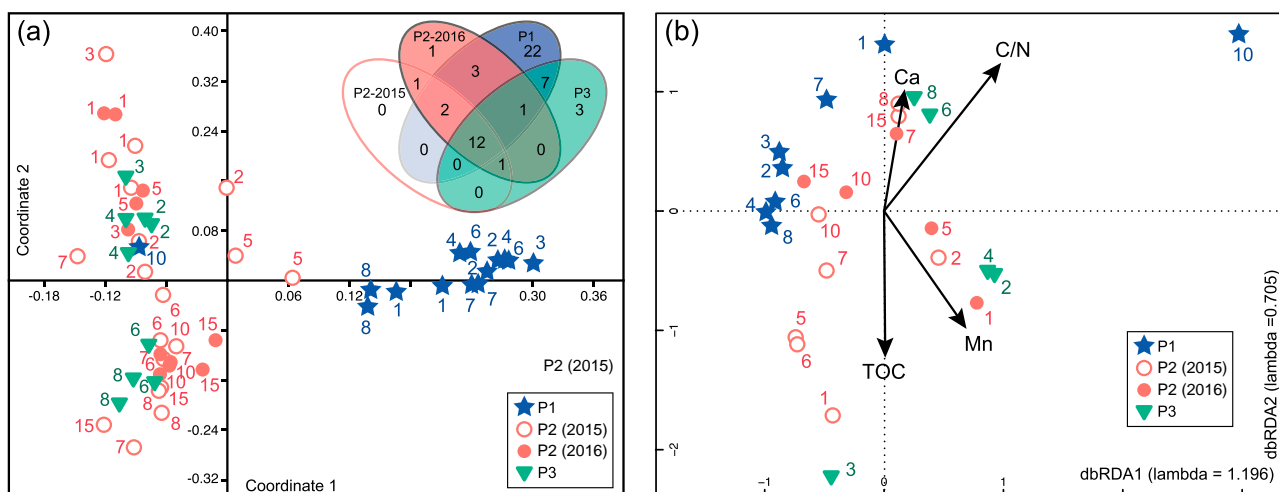


Figure 6. Statistical analysis of the microbial community based on *mcrA* structure analysis: (a) PCoA and Venn diagram based on T-RFLP described OTUs (of *mcrA* gene) for the 3 sites in Petrozavodsk Bay; (b) NMDS of TRFs combined to a distance-based redundancy analysis of associated environmental parameters using step-across dissimilarities and permutation test under reduced model (999 permutations). Only significant variables were plotted on the dbRDA.

Results from genotyping of the *mcrA* gene showed a functional community structure difference between site P1 and the 2 other sites, P2 (independently of the sampling year) and P3 (Fig. 6a; ANOSIM significance at $p < 0.0002$). All samples generated 53 different OTUs. For 2016, a higher richness was observed for P1 (41 OTUs for P1, 21 for P2, and 24 for P3; Fig. 6b). P1 exhibited a large number of unique OTUs (22) and a strong difference in the overall composition of its community, in particular for the samples between 1 and 8 cm. The 2 other sites did not show particular differences between each other as they shared 14 OTUs, and only 2 had unique OTUs at P2 and 3 at P3. All OTUs from P2-2015 were shared with P2-2016, and most OTUs were shared with the 2 other sites (15 of 16). A secondary clustering was observed within the P2-P3 cluster; shallow samples (1–5 cm) differed significantly in their structure from deeper samples (6–15 cm; ANOSIM $p < 0.001$). Samples from 2015 (P2 only) tended to slightly blur this dichotomy as samples between 3 and 7 cm were scattered between these 2 marked groups.

For the functional dataset, “site” was found to be a significant parameter ($p = 0.002$) characterizing the functional communities, confirming the ANOSIM results; however, depth was not found to be significant. Sediment Mn ($p = 0.002$), Ca ($p = 0.002$), TOC ($p = 0.002$), and C/N ($p = 0.026$) content were identified as the structuring parameters of the functional community.

Functional community analysis: sequences

We separated 328 usable sequences (39 chimeras of 367 sequences) into 73 OTUs (95% similarity). These OTUs

were generally related to uncultured methanogenic Archaea. Based on the obtained phylogenetic tree, they form several branches, mainly related to the Methanomicrobia class (68 OTUs). Only 5 OTUs were attributed to the Methanobacteria class.

Within Methanomicrobia, 51 OTUs were grouped into a poorly constrained cluster named the Onego group (Fig. 7). Closely related sequences were associated with the former Fen cluster (Supplemental Material) and were classified either into unclassified Methanoregulaceae, unclassified Methanomicrobiales, or unclassified Euryarchaeota. Other sequences were attributed to Methanosarcinaceae (8 OTUs) and were identified mainly at site P2. Five OTUs seem to be related to sequences identified as members of the *Methanolinea* genus. The rest of the affiliated Methanomicrobia sequences grouped with members of the Methanocellales order (4 OTUs). The 5 remaining OTUs grouped within a Methanobacteriales group and were retrieved mainly from the rare OTUs pool (PP). *In silico* T-RFLP and site-specific cloning libraries allowed us to attribute site occurrence to 51 OTUs (color-coded in Fig. 6). Five OTUs were identified at site P1 only, all of which belonged to the Onego cluster (5 OTUs). Ten OTUs from the Onego cluster, 5 *Methanosarcina*, 1 *Methanocella*, and 1 Methanobacteria were found at P2 only. Site P3 specific OTUs were attributed to the Onego cluster (3 OTUs) and to *Methanolinea* (1 OTU). Based on cloning results, phylogenetic distance measured by Unifrac was found to be higher between P1 and P2 (0.68) or between P1 and P3 (0.64) than between P2 and P3 (0.59). All measured distances were found to be significant ($p < 0.001$). Finally, note that no anaerobic oxidation of methane (ANME) sequence was identified.

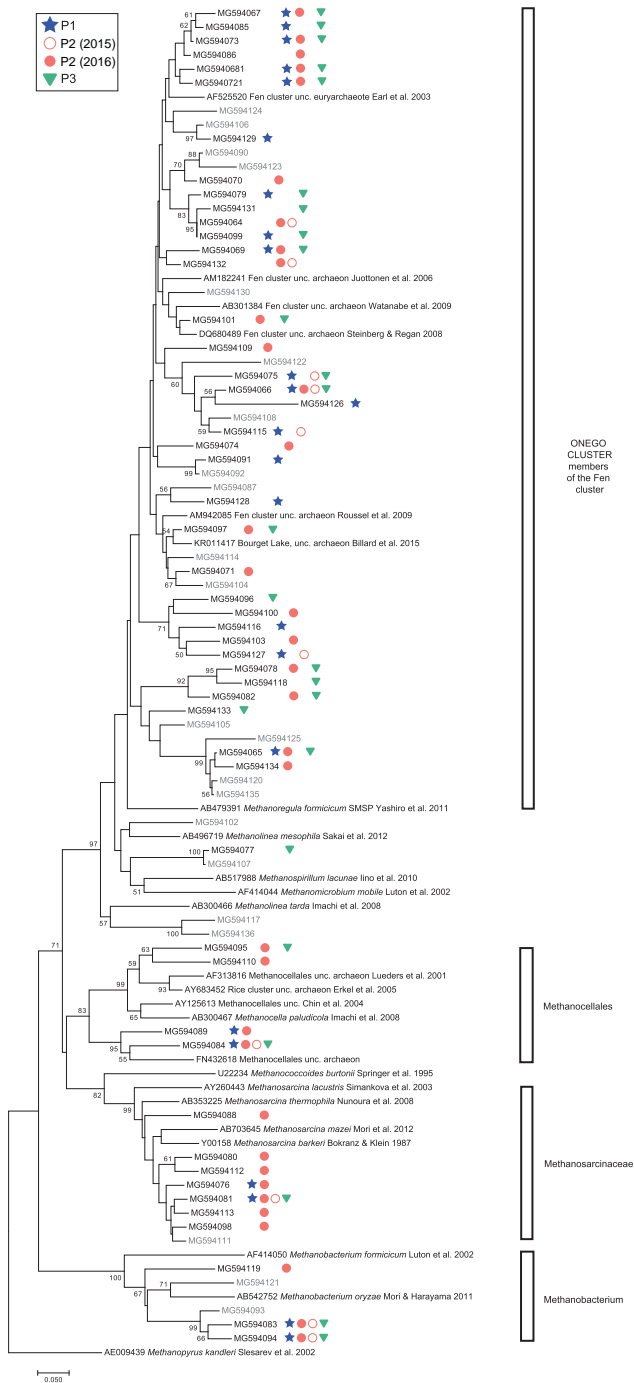


Figure 7. *McrA*-based phylogenetic tree and occurrence (supported by *in silico* TRFs) at the sampling sites P1, P2, and P3.

Methanotrophic community from 16S rRNA gene sequencing and drivers of its structure

At P2, sequences related to families known to perform aerobic oxidation of CH_4 were obtained at all depths between 1 and 15 cm (Table 4); however, higher read abundances were observed between 1 and 8 cm. In particular, reads assigned to the Methylophilaceae family were >1% of the total read within this interval. Reads

associated with the Methylococcaceae family reached 2.7% at 5 cm (*Methylobacter* genus accounting for 2.5%). Methylobacteraceae were also found, but at abundances <0.2%. Reads associated with the anaerobic methanotrophs *Cand. Methyloirabilis* ranged between 0.6 and 1.5% in the first 6 cm and attained 3.3% at 6 cm, 1.8% at 7 cm, and decreased to 0.5% below 9 cm. Archaeal *Cand. Methanoperedens* reads reached 0.6–0.7% at 6–7 cm. No other ANME sequence could be identified within the library.

Hierarchical clustering constrained by sediment depth obtained a cophenetic correlation of 0.77 and allowed us to decipher 3 main clusters (Fig. 8) between 1 and 4 cm, 6 and 8 cm (Morisita similarity >0.9 for both), and 9 and 10 cm (Morisita similarity of ~0.9). Sample 5 was identified as an outlier and was removed from the analysis. The 15 cm sample did not show strong similarities with the others. For the 16S microbial dataset, no parameter was found to significantly structure the community.

Discussion

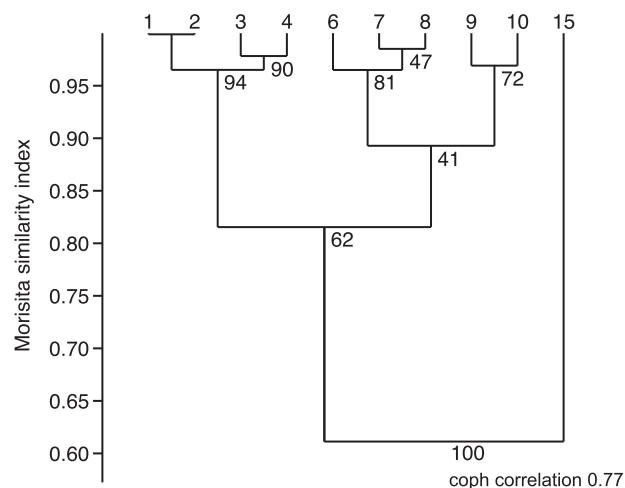
Methane production and oxidation along the bay transect

Although CH_4 concentration profiles displayed similar diffusive patterns along the transect in Petrozavodsk Bay, the absolute concentrations varied broadly. Site P1 exhibited much higher CH_4 concentrations, both in the sediment down to 15 cm and at the sediment–water interface (0 cm depth, which corresponds to the first millimeter of sediment), than P2 and P3 (Fig. 4a). Methane diffusive flux was >6 times higher at P1 than at P2 and >12 times than at P3 (Fig. 4a). This horizontal trend among the 3 sites was also observed for potential CH_4 production (Table 3) as well as for the maximum *mcrA* gene copy numbers (Fig. 5a), and fairly supported by ANOSIM results. The highest CH_4 production at P1 was characterized by the maximum *mcrA* gene copy number measured among all 3 sites (1.4×10^7 copies g^{-1} DW). At P3, the overall *mcrA* profile remains below 1000 copies of *mcrA* g^{-1} DW, suggesting a low methanogenic community presence associated with lower CH_4 concentrations.

Overall, the values observed for the Petrozavodsk Bay of Lake Onego were all several orders of magnitude lower than those observed in other relatively large lakes of similar mesotrophic state, such as Lake Geneva (10^6 to 10^7 *mcrA* copies g^{-1} DW; Fuchs et al. 2016) or Lake Kinneret (10^5 to 7.0×10^6 *mcrA* copies g^{-1} DW; Bar-Or et al. 2015). Methane concentrations were also generally lower than those observed in Lake Geneva. As an example, the Shuya River-related site P1 showed similarities in

Table 4. Identified methanotrophic families and relative read abundance through 16S rRNA gene sequencing at site P2 in 2015.

Family	1 cm	2 cm	3 cm	4 cm	5 cm	6 cm	7 cm	8 cm	9 cm	10 cm	15 cm
Aerobic methane oxidation											
Methylobacteriaceae	0.21	0.18	0.19	0.18	0.04	0.19	0.09	0.10	0.07	0.07	0.15
Methylophilaceae	2.94	2.67	1.89	2.69	1.46	2.15	1.78	1.26	0.23	0.13	0.22
Methylococcales CABCE06	—	—	—	—	0.16	—	—	—	—	—	—
Methylococcales <i>Crenothrix</i>	0.15	0.15	0.21	0.25	0.04	0.25	0.26	0.09	0.01	0.04	0.06
Methylococcales <i>Methylobacter</i>	0.17	0.12	0.11	0.12	2.49	0.39	0.18	0.16	0.02	0.01	0.03
Methylococcales Methylococaceae unknown genus	—	—	—	—	0.01	—	—	—	—	—	—
Methylococcales pIW-20	0.01	—	—	—	0.01	—	—	0.01	—	—	—
All Methylococcales	0.33	0.27	0.32	0.38	2.70	0.64	0.44	0.26	0.03	0.05	0.09
Anaerobic methane oxidation											
<i>Candidatus Methanoperedens</i>	—	0.02	0.03	0.05	0.03	0.71	0.61	0.20	0.04	0.06	0.48
<i>Candidatus Methylopirabilis</i>	1.11	0.89	1.49	1.35	0.63	3.33	1.83	1.03	0.46	0.56	0.29
total reads per sample	12,969	8435	13,607	28,428	51,894	14,810	12,526	17,947	17,704	20,779	22,577

**Figure 8.** Constrained hierarchical clustering of P2-2015 samples based on the methane-related 16S rRNA gene sequences.

concentrations to deeper (50–60 m) and inactive areas of the Rhone delta in Lake Geneva (Sollberger et al. 2014, Randlett et al. 2015) or to the trenched sediment of the central basin (Brandl et al. 1993), which are all much deeper than P1 sediment cores (90–250 m). Lake Onego and the atypical Petrozavodsk Bay are thus relatively small CH₄ producers, in particular during winter. Concentrations of CH₄ in the water column that were close to detection limits support this statement. Average CH₄ production potential at P1 in the first 15 cm was, however, higher than that measured in Lake Geneva and Lake Stechlin at 4°C between 15 and 25 cm (Fuchs et al. 2016). These differences could be explained by the shallower and more river influenced setting of Lake Onego's site P1. By contrast, mean CH₄ production values at P2 and P3 were similar to or slightly lower than observed in Lake Geneva, Lake Stechlin (Fuchs et al. 2016), and in most small Swedish lakes studied by Duc et al. (2010) for 4°C incubation experiments.

While large differences were observed for methanogenesis between site P1 and the 2 other sites (Fig. 6), methanotrophy seemed to more evenly distributed based on *pmoA* copy numbers (Fig. 5b). The maximum number of *pmoA* copies was slightly higher at P1, but quantities were of the same order of magnitude and followed similar distribution above 7 cm. This finding suggests a relative deficiency of methanotrophic activity at sites P2 and P3 compared with P1. The potential rates of CH₄ oxidation were also higher for P1 (1350–1425 ng CH₄-C g⁻¹ DW h⁻¹), whereas rates measured for P2 and P3 remain generally below 1000 ng CH₄-C g⁻¹ DW h⁻¹, except for the top centimeters of site P3 (1163 ng CH₄-C g⁻¹ DW h⁻¹; Table 3b). These rates are similar to those calculated for Lake Geneva but are much lower than

those calculated for Lake Stechlin (Fuchs et al. 2016) over 24 h.

In summary, CH₄ production was higher in the sediments of Petrozavodsk Bay that were closer to the river. Methane consumption was also higher in P1, but to a lesser extent than other sites. Calculations based on isotopic ratios showed that only 20% of the produced CH₄ was consumed in the top 15 cm of sediments at P1 while methanotrophic communities consumed up to 80% in P2 and P3 (when a closed system was considered), highlighting the difference in CH₄ cycling along the bay (discussed later).

Links between community structure and methane cycling along the bay transect

Methanogenic community in Lake Onego

Sequencing of the *mcrA* gene revealed an overall dominance of hydrogenotrophic methanogenic OTUs Methanoregulaceae, Methanocellaceae, Methanobacteriaceae, and Methanomicrobiaceae (Fig. 7). The only sequences obtained from known acetoclastic organisms belonged to the Methanosarcinaceae order. Methanocellales members are more common in relatively warm environments, such as tropical lakes (Conrad et al. 2007) or rice paddies (Sakai et al. 2008, 2010). They are rarely detected in freshwater environments without enrichment (Borrel et al. 2011), but their preference for low H₂ concentrations prevalent in most freshwater lakes may explain their retrieval in the Onego library (Conrad et al. 2006, Sakai et al. 2009).

Methanobacterium have been retrieved from lakes with high carbon supply, such as in a dystrophic acidic lake (Chan et al. 2002) or hypereutrophic Lake Priest Pot (Earl et al. 2003). Petrozavodsk Bay can be characterized as dystrophic, but it does not exhibit acidic conditions.

Methanomicrobiales have also been identified in sub-oxic to anoxic sediments of carbon-rich ponds (Bri e et al. 2007), where they were found associated with Methanosarcinales, an association that generally dominates lacustrine sediment methanogenic clone libraries (Borrel et al. 2011). Here, acetoclastic *Methanosarcina* seems to outcompete the other acetoclastic clade *Methanosaeta*, more commonly in lake environments where low acetate concentrations are found (Jetten et al. 1992). *Methanosarcina* have been shown to be better adapted to low temperatures; they were abundant at 4 °C compared to *Methanosaeta*, which was dominant at 20 °C (Steinberg and Regan 2009), potentially explaining their occurrence in the present study. The cold temperature in Lake Onego sediment should also discriminate against hydrogenotrophic methanogens, shown in the

past to be less adapted to cold environments than acetoclastic methanogens (Schulz and Conrad 1996). The important diversity of hydrogenotrophic organisms in Lake Onego's sediment, however, may be favored by the age and poor lability of the OM (Conrad 2005) dominating the sediment of Lake Onego (Tekanova 2012). The CH₄ production zone in Lake Onego is relatively deep. The δ¹³C_{CH4} below 10 cm, where CH₄ production seems to be most intense, was relatively heavy at all 3 study sites. Such signatures have been observed for environments where acetoclastic methanogenesis is inhibited (Conrad et al. 2009), which tends to support the dominance of methanogenesis from H₂/CO₂ in the deepest measured layers of the Petrozavodsk Bay sediments.

Characteristics of site P1 functional community

Site P1 hosts a singular functional community (Fig. 6a). T-RFLP fragments from *mcrA* show 22 singular OTUs represented only at P1 (Fig. 6a), but they could not be unequivocally identified. Cloning and sequencing results, combined with *in silico* TRFLP characterization, allow identification of some sequences related to hydrogenotrophic *Methanoregula*/Fen cluster. Other sequences only found at P1 remain unclassified. Members of the Methanoregulaceae family, originally known as Fen cluster organisms (Galand et al. 2002), were identified in shallow sediments of Finnish oligotrophic fens. They are common in freshwater lakes, and in particular in those harboring relatively acid conditions observed in peats or fens (Galand et al. 2002, Cadillo-Quiroz et al. 2008). The high humic substance load of the Shuya River feeding into Petrozavodsk Bay (Sabylina et al. 2010, Belkina 2011) may explain the high richness of this group in the Onego sediment (72 OTUs of 97).

The specific functional community at P1 is associated with a larger community and greater metabolism of the CH₄ cycle (Fig. 6). Statistical comparison with the potential of CH₄ production was not possible because too few samples were measured, but the rates of production were largely higher at P1 than at other sites (Table 3a), which is also the case for *mcrA* copy numbers (ANOSIM test with $p > 0.08$ between P1 and P2, and $p > 0.006$ between P1 and P3). As a consequence, CH₄ production largely exceeded CH₄ consumption, resulting in a significantly different isotopic signature of CH₄-C (Table 2, Fig. 4b). Site P1 was characterized by a higher C/N ratio in its sedimentary column (Fig. 3). The distance-based RDA of the functional community against the sedimentary parameters of the 3 sites identified this parameter as a contributor to this spatial heterogeneity. The C/N ratio is a proxy of the terrestrial versus lacustrine origin of the OM. The increased relative nitrogen content in

bacterial and algal microorganisms ($C/N < 10$) compared to terrestrial plant debris ($C/N > 30$) was used to trace the origin of sedimentary OM (Meyers 1994). The Shuya River contributes an important quantity of OM to Petrozavodsk Bay (Kalinkina et al. 2013), reflected by the higher turbidity caused by the load of humic substances in the lake close to its mouth and high C/N ratios in its waters (Table 1). The highest C/N ratio measured in sediment P1 clearly demonstrates an enrichment in terrestrial organic carbon compared to P2 and P3 (Meyers 1994). The specific organic content of the sediments at P1 (compared to P2 and P3), likely enriched in riverine inputs, may also contain heavier OM (higher $\delta^{13}C_{OM}$, not measured here), which could be reflected in the heavier $\delta^{13}C_{CH_4}$ values measured in the deepest layers (15 cm) of that site (Fig. 3b). However, the large $\delta^{13}C$ ranges exhibited by terrestrial plants, soil humic substances, and freshwater algae often prevent the identification of OM sources through this method (Schiff et al. 1990). Our work mainly explained this difference by the dominance of methanogenesis over methanotrophy in P1, masking the progressive contribution of methanotrophy to CH_4 -C fractionation.

Our statistical analysis also revealed that Mn is a structuring parameter of the *mcrA* community, which is particularly enriched in P1 (Fig. 3b and 6b). Mn behaved differently from Fe, Ca, and all other elements directly influenced by riverine inputs (Fig. 3b). Because Mn is solubilized more rapidly in reducing conditions than Fe (Wersin et al. 1991, Boyle 2002), we interpreted lower Mn quantities in P1 as an indicator of more reducing conditions in the sediment, allowing the element to remain solubilized. These reducing conditions are also reflected in the higher Fe/Mn ratio for P1 (Fig. 3a) than for P2 and P3. We suggest that more reducing conditions prevail in P1 while P2 and P3 exhibit relatively profound oxygen penetration (down to 7 cm) that naturally influences the CH_4 cycle. This differential O_2 penetration is likely caused by the higher intensity of microbial activity in P1, which may be induced by higher nutrient inputs (Sabylina et al. 2010) by the river at this site than the 2 other sites. West et al. (2016) showed a direct correlation between primary production and sediment methanogenesis rates in lakes. The inflowing water brings in nutrients (Sabylina et al. 2010) that could fuel the primary production of the lake and subsequently lead to higher methanogenic rates or respiration rates once autochthonous OM gets buried. Increased content of Fe and TN in P1 and their maximal concentrations in the Shuya River support this hypothesis (Table 1); however, some unknowns remain regarding the horizontal mixing of water within the bay. Minimum concentrations of TOC and Fe in the deepest layers of the

lake at each site, accompanied by smaller color indexes, would suggest that Shuya River water flows on top of lake water. Potentially, another source of water (likely runoff from the urbanized area) may also influence the deeper waters through, for example, high nitrogen content. This hypothesis is currently being investigated by companion studies.

Overall, our data suggest that the CH_4 cycle at P1 differs from P2 and P3 because of the strong effect of this riverine input at the mouth of the Shuya River. This input and all the resulting spatial characteristics discussed earlier sustain at P1 a functional community that differs from P2 and P3 both in structure and abundance, implying a higher methanogenic activity that exceeds methanotrophy. The lower methanotrophy in P1 might be associated with more reducing conditions, which prevent an efficient establishment of aerobic methanotrophy in the sedimentary column. However, CH_4 concentrations in the water column are not higher at this site than the others. Hence, CH_4 oxidation likely occurs in the uppermost few millimeters of sediment, which may have been missed by our sampling. The oxidative condition in which incubations have been realized show that CH_4 oxidation potential exceeds those of other sites and could account for a complete oxidation of the CH_4 produced in the sediment. More work is needed to understand why methanotrophy is limited in this site.

Methane production and consumption in the sedimentary column

Methane production

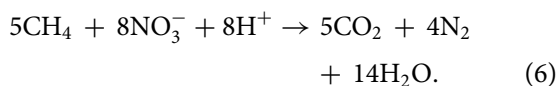
Concentrations of CH_4 along the Petrozavodsk Bay transect show similar diffusive profiles but with notably different rates (Fig. 4a). They also suggest a deep zone of CH_4 production, potentially below the measured sediment depths. Actual CH_4 production zones can be tracked through the decrease of $\delta^{13}C$ isotopic signature of biogenic CH_4 observed in Lake Onego with depth. Increased concentrations with depth and characteristic isotopic signatures of biogenic CH_4 (around -84% at P2 and P3; Whiticar 1999), likely related to the dominant hydrogenotrophic methanogenesis pathway (Conrad et al. 2009), imply that most of the CH_4 production occurs below 10 cm (Fig. 3b). This finding is also indicated by the CH_4 production potentials observed at P3, which begins to be measurable in the 10–15 cm interval (Table 3). These data suggest even deeper CH_4 production zones, possibly fueled by long-term accumulation of OM and its recycling by deep methanogenic groups. Interestingly, recent seismic surveys in Petrozavodsk Bay highlighted the presence of gas escape structure in the deep Onego sediment (D. Subetto, pers.

comm.). Deeply buried layers could fuel heterotrophic microbial communities on geological time scales (Parkes et al. 2005) and result in the slow diffusion of CH₄ to the surface. Our results show that our sampling only touches the most surficial processes of this CH₄ cycling.

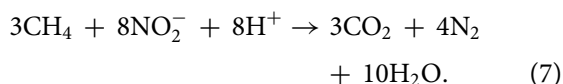
Anaerobic methane oxidation

The CH₄ produced diffuses upward in the sediment, as seen in the typical shape of the CH₄ concentration profiles, and starts to be oxidized at 7 cm at P2 in 2016 (10 cm in 2015) and 11 cm at P3. The $\delta^{13}\text{C}_{\text{CH}_4}$ (Fig. 4a–b) increases correspondingly from about -84‰ to less than -60‰ (Holler et al. 2009). Given the large O₂ penetration (down to at least 5 cm) in the core of P2 and P3, this type of shift can be caused by aerobic and anaerobic oxidation of CH₄ in these layers (Whiticar and Faber 1986). The anaerobic methanotrophs *Cand. Methanoperedens* identified in relatively high abundance at 6–8 cm at P2 (Table 4) harbor the full *mcrA* subunit (Haroon et al. 2013) and could cause such a fractionation signature (Fig. 4b) and the relatively high *mcrA* gene copy number observed above 10 cm at P2 and P3 (Fig. 5a). The co-occurrence of *Cand. Methyloirabilis* (identified by their 16S rRNA gene sequences) in the same interval (Table 4) could enhance this AOM and would maintain high *pmoA* copy numbers between 5 and 10 cm at P2 and potentially P3 (Luesken et al. 2011).

Haroon et al. (2013) suggested that *Cand. Methanoperedenaceae* could perform AOM using nitrate as the terminal electron acceptor via the reverse methanogenesis pathway:



A complementary process was also acknowledged because the nitrite produced was shown to be reduced by *Cand. Methyloirabilis oxyfera* into N₂ (equation 7), allowing a second step of CH₄ oxidation (Haroon et al. 2013). This CH₄ oxidation pathway was described by Ettwig et al. (2010) as an intraaerobic nitrite reduction pathway:



The identified 16s rRNA sequences of *Cand. Methanoperedens* and *Cand. Methyloirabilis*, together with the $\delta^{13}\text{C}_{\text{CH}_4}$ and simultaneous functional gene abundances, provide an example of active anaerobic oxidation of CH₄ at site P2 (and potentially site P3, given the functional community similarities; Fig. 6a). Based on the specific association to nitrate and nitrite reduction

observed for this consortium, AOM might be coupled to the N cycle in Lake Onego; however, our data cannot confirm this pathway, and AOM associated with Mn or Fe cannot be ruled out. Recent work shows that a member of the *Candidatus* Methanoperedenaceae family is associated with Fe-supported AOM (Cai et al. 2018). Thorough analysis of our *mcrA* or 16S rRNA sequences failed to identify other ANME sequences. This work is to our knowledge the first time that a *Cand. Methanoperedens* and *Cand. Methyloirabilis* association has been described in a natural environment, and in particular in lake sediments (Welte et al. 2016). Our findings suggest the relative importance of (nitrate-dependent) anaerobic oxidation of CH₄ in freshwater systems and establish Lake Onego as an ideal site for the study of anaerobic oxidation of CH₄ in freshwater lake sediments. Tracking the fate of potential electron acceptors such as nitrate in the sediment pore water could help verify the prevalent AOM pathway in Petrozavodsk Bay.

Aerobic methane oxidation

Sequences related to Methylobacteriaceae, Methylophilaceae, and Methylococcales were obtained from site P2. Betaproteobacteria Methylophilaceae-related sequences dominated the methanotrophic community and accounted for almost 3% of the total 16S rRNA gene sequences obtained at 1 cm sediment depth at P2 (Table 1), where the CH₄ consumption potential was maximal (Fig. 4). Sequences associated with the Gammaproteobacteria Methylococcales order reached 2.7% of the total number of reads at 5 cm (mainly members of the *Methylobacter* genus) but otherwise remained below 0.4% in the upper 5 cm and below 0.7% between 6 and 8 cm. Below 8 cm, sequences associated with organisms performing aerobic oxidation of CH₄ never exceeded 0.23% of the total reads, which corresponded to the decrease observed for *pmoA* copies numbers (Fig. 5b). Members of the Methylococcaleae family were recovered in low temperature environments (Sundh et al. 2005), in particular the dominant genus *Methylobacter* observed at 5 cm (e.g., Warttinen et al. 2006, Svenning et al. 2011). They were shown to also be active in anoxic conditions (e.g., Oswald et al. 2016), which could explain their occurrence below 5 cm in the cold sediments of Lake Onego. Methylophilaceae members are facultative methylotrophs (He et al. 2012). By relying both on CH₄ and methanol, they could be favored in competition for substrate. Based on phylogenetic data, co-occurrence of anaerobic and aerobic CH₄ oxidizers was observed below 6 cm. There, Methylophilaceae

could effectively rely on less valuable substrate not targeted by other obligate methanotrophs.

Vertical structure of the methane cycle

The structure obtained from *mcrA* fingerprinting showed significant clustering (both for P2 and P3) between samples from 1 to 5 cm and from 6 to 15 cm (Fig. 6a and ANOSIM pairwise significance, $p < 0.001$). Comparatively, the 16S rRNA gene sequences (Table 4) and clustering (Fig. 8) showed that the upper 5 cm was mainly composed of aerobic methanotrophs, together with some *Cand. Methylophilum mirabilis* sequences. Below this, the number of AOM-related sequences increased and defined a second cluster, where aerobic and anaerobic CH₄ oxidizer sequences cohabitate. At 15 cm, the number of sequences associated with aerobic methanotrophs drastically decreased, and more *Cand. Methanoperedens* sequences were observed.

Based on our multivariate analysis, 4 parameters played a significant role in structuring the functional *mcrA* community. The first is the redox sensitive Mn. Based on its variation, its independence from other elements, and the deep O₂ penetration in cores P2 and P3 (down to 5 cm minimum), its redox sensitivity marked clear redox boundaries at 6 cm at P2 and P3 (Fig. 3a and 6b). Two other structuring variables were TOC and Ca, which were highly influenced by riverine inputs into the bay and decreased sharply at 6 cm (Fig. 3a). Ca behaved similarly to Fe and Ti (Fig. 3). The Fe and Ti marked changes in the content of detrital fractions, and therefore changes in terrestrial inputs with time. In the bay, the TOC content was mainly influenced by the Shuya River (Sabylina et al. 2010) because the lake overall exhibited relative low primary production compared to its allochthonous inputs of OM (Kalinkina et al. 2013). An important feature of the TOC profile in Onego was the strong changes imparted to human activity in the river and lake catchment area. In the late 1970s and early 1980s, intense deforestation, farmland ameliorative work, and ploughing strongly enriched the Shuya River catchment with OM (Sabylina et al. 2010), hence contributing to the currently observed high concentrations in the uppermost centimeters of the sedimentary column (Fig. 3a). We therefore suggest that the redox boundary and human influence on the quantity and origin of the OM (and terrestrial inputs in general) imposed this sharp transition between the 2 functional communities found at P2 (and potentially P3). Below 5 cm, CH₄ production coexisted with AOM. Above 5 cm, oxidative conditions existed with little to no CH₄ production (although methanogen sequences could be retrieved) and higher degradation rates (Table 3). Moreover, a boundary at 10 cm was observed from clustering of the 16S community structure

and likely marks the lower limit for AOM and the dominance of CH₄-producing communities below that depth (Fig. 8, Table 4). The C/N ratio also had a structuring effect on *mcrA* communities, mainly because of the differentiation of site P1 from sites P2 and P3, and was a function of the fraction of terrestrial versus lacustrine OM in the sediment, as explained earlier.

Based mainly on P2 data, the CH₄ cycle vertical structuration can be described as follows:

- (1) Between 1 and 5 cm: high CH₄ isotopic signatures, high *pmoA* gene copy numbers, high CH₄ consumption rates altogether support dominance of methanotrophy in oxygenated environments. Aerobic methanotrophic taxa like Methylophilaceae and Methylococcales members identified by 16S rRNA gene sequences (Table 4) likely carry out this process.
- (2) Between 6 and 10 cm: increase in *mcrA* genes and transitional carbon isotopic signatures likely relate to oxidation of CH₄. The co-occurrence of aerobic and anaerobic CH₄ oxidizers with CH₄ producers suggests a transitional zone between CH₄ production and oxidation. AOM likely starts to occur in this relatively thick layer.
- (3) Below 10 cm: higher CH₄ concentrations are associated with an increase in relative abundance of CH₄ producers belonging to the hydrogenotrophic Methanoregulaceae family. The number of *pmoA* copies decreases with the relative abundance of sequences of aerobic CH₄ oxidizers while *mcrA* copy numbers remain relatively high. We expect this sediment to host CH₄ production, but this supposition is not directly supported by potential CH₄ production but rather might be caused by the limitations inherent to the incubation method, for example an enhanced CH₄ consumer efficiency in the lab experiment. Interestingly, *Cand. Methanoperedens* sequences are still high in those layers. We do not know if these organisms participate in AOM or if they contribute to CH₄ production as suggested by Lloyd et al. (2011).

Conclusion

Methane concentrations and isotopic composition suggest an active CH₄ cycle in the sediments of Petrozavodsk Bay of Lake Onego but with strong spatial variations along the bay. The shallowest site, and also the most affected by the Shuya River (P1), has a singular functional community associated with higher CH₄ production potential, higher CH₄ flux rate, and higher number of *mcrA* copies. Methanotrophy at that location

seems relatively less important. The methanogenic community is characterized by poorly known members of the Methanoregulaceae Fen cluster that are likely better adapted to the higher terrestrial/allochthonous OM inputs that characterize this site. The production potential and the sediment fluxes of CH₄ decrease while the methanogenic communities vary moving away from the river mouth toward the open lake. Higher *Methanosarcina* diversity is observed in the center of the bay, although members of the Fen cluster are still present, together with *Methanocella* and *Methanobacterium* members. The 16S rRNA gene sequences obtained from sediments of the middle of the bay signal the presence of an AOM community likely supported by nitrate and nitrite reduction, which is concentrated between 5 and 10 cm of the core. At this site, and further in the open lake, all the produced CH₄ seems to be oxidized. Below 10 cm, hydrogenotrophic methanogenesis might be the dominant process. Our approach, which couples biogeochemical and sedimentological analysis with analysis of functional and diversity traits of the microbial community partly untangles the complexity of the sedimentary environments. Our analysis identifies riverine inputs and sediment oxygenation as important factors in the spatial structure, intensity, and nature of the sedimentary CH₄ cycle in Petrozavodsk Bay. Clear distinction between CH₄ production and CH₄ degradation zones have been observed and are overlapped by a transitional interval potentially hosting nitrogen-supported AOM. The heterogeneity of the CH₄ cycle in large lakes is demonstrated in this study, with strong intrinsic differences in sedimentary characteristics (amount of allochthonous inputs) resulting in changes of communities that impact CH₄ production (8–200 ng CH₄-C g⁻¹ h⁻¹) and fluxes to the water column (0.5–6 mmol m⁻² d⁻¹). These changes occur at the bay scale within a range of a few kilometers at depths varying from 10 to 27 m. Because they were measured during the ice-covered period, they most likely represent a minimum for the year, meaning that the observed heterogeneity may be exacerbated during more productive periods. When possible, the integration of these variations within global CH₄ budget models will likely help reduce the uncertainty inherent to such estimations.

Competing interest

The authors declare no conflict of interest.

Acknowledgements

This work was supported by the FEEL foundation, “Life Under the Ice project” (<http://wiki.epfl.ch/ladoga>). We are

grateful to the INRA MIGALE bioinformatics platform (<http://migale.jouy.inra.fr>) for providing help, support, and computational resources. The authors also thank the Limnology Center from EPFL for funding this research, and the Northern Water Problems Institute of Russian Academy of Sciences, as well as Mischa Haas and Alois Zwysig (EAWAG) for providing technical and logistical support during field expeditions. The authors also thank Elodie Rumiano, Cécile Chardon, Nathalie Tissot, and Jérôme Jean-denand (UMR CARRTEL) for molecular biology work; Stéphane Pesce and Christophe Rosy (IRSTEA) for methane measurements during incubations; Thomas Junier (EPFL) for his help with TRiFLe; and Phanélie Berthon (LIBM) for kindly providing a dry-shipper for field work. Finally, we thank Hannah Chmiel (EPFL) and Daniel Ariztegui for their contribution to field operations and workshops. The helpful and valuable comments of the 2 anonymous referees improved the manuscript.

ORCID

Camille Thomas  <http://orcid.org/0000-0002-7651-2542>
 Hilmar Hofmann  <http://orcid.org/0000-0001-6140-5886>
 Nathalie Dubois  <http://orcid.org/0000-0003-2349-0826>
 Natalia Belkina  <http://orcid.org/0000-0002-9928-022X>
 Mariya Zobkova  <http://orcid.org/0000-0002-8106-3665>

References

- Altschul SF, Gish W, Miller W, Myers EW, Lipman DJ. 1990. Basic local alignment search tool. *J Mol Biol.* 215: 403–410.
- Bar-Or I, Ben-Dov E, Kushmaro A, Eckert W, Sivan O. 2015. Methane-related changes in prokaryotes along geochemical profiles in sediments of Lake Kinneret (Israel). *Biogeosciences.* 12:2847–2860.
- Bastviken D, Cole J, Pace M, Tranvik L. 2004. Methane emissions from lakes: dependence of lake characteristics, two regional assessments, and a global estimate. *Glob Biogeochem Cy.* 18:1–12.
- Bastviken D, Ejlertsson J, Tranvik L. 2002. Measurement of methane oxidation in lakes: a comparison of methods. *Environ Sci Technol.* 36:3354–3361.
- Belkina NA. 2011. Role of sediments in the processes of transformation of organic matter and nutrients in lake ecosystems. In: *Transactions of Karelian Research Centre of the Russian Academy of Science, Petrozavodsk, Russia. Karelian Research Center Russian Academy of Science, Series Limnology.* 4:35–41. Russian.
- Belkina NA, Ryzhakov AV, Timakova TM. 2008. Transformation of petroleum hydrocarbons in sediments of Lake Onego. *Proceedings of the Taal 2007 12th World Lake Conference*; p. 2191–2196.
- Billard E, Domaizon I, Tissot N, Arnaud F, Lyautey E. 2015. Multi-scale phylogenetic heterogeneity of archaea, bacteria, methanogens and methanotrophs in lake sediments. *Hydrobiologia.* 751:159–173.
- Bokranz M, Klein A. 1987. Nucleotide sequence of the methyl coenzyme M reductase gene cluster from *Methanosarcina barkeri*. *Nucleic Acids Res.* 15:4350.

- Bolger AM, Lohse M, Usadel B. 2014. Trimmomatic: a flexible trimmer for Illumina sequence data. *Bioinformatics*. 30:2114–2120.
- Borrel G, Jézéquel D, Biderre-Petit C, Morel-Desrosiers N, Morel JP, Peyret P, Fonty G, Lehours AC. 2011. Production and consumption of methane in freshwater lake ecosystems. *Res Microbiol*. 162:833–847.
- Bouffard D, Zdorovenov RE, Zdorovenova GE, Pasche N, Wüest A, Terzhevik AY. 2016. Ice-covered Lake Onega: effects of radiation on convection and internal waves. *Hydrobiologia*. 780:21–36.
- Boyle JF. 2002. Inorganic geochemical methods in palaeolimnology. In: *Tracking environmental change using lake sediments*. Springer; p. 83–141.
- Brandl H, Hanselmann KW, Bachofen R, Piccard J. 1993. Small-scale patchiness in the chemistry and microbiology of sediments in Lake Geneva, Switzerland. *J Gen Microbiol*. 139:2271–2275.
- Brankovits D, Pohlman JW, Niemann H, Leigh MB, Leewis MC, Becker KW, Iliffe TM, Alvarez F, Lehmann MF, Phillips B. 2017. Methane-and dissolved organic carbon-fueled microbial loop supports a tropical subterranean estuary ecosystem. *Nat Commun*. 8.
- Bri e C, Moreira D, L opez-Garc a P. 2007. Archaeal and bacterial community composition of sediment and plankton from a suboxic freshwater pond. *Res Microbiol*. 158:213–227.
- Cadillo-Quiroz H, Yashiro E, Yavitt JB, Zinder SH. 2008. Characterization of the archaeal community in a minerotrophic fen and terminal restriction fragment length polymorphism-directed isolation of a novel hydrogenotrophic methanogen. *Appl Environ Microbiol*. 74:2059–2068.
- Cai C, Leu AO, Xie G-J, Guo J, Feng Y, Zhao J-X, Tyson GW, Yuan Z, Hu S. 2018. A methanotrophic archaeon couples anaerobic oxidation of methane to Fe(III) reduction. *ISME J*. 12:1929–1939.
- Chan OC, Wolf M, Hepperle D, Casper P. 2002. Methanogenic archaeal community in the sediment of an artificially partitioned acidic bog lake. *FEMS Microbiol Ecol*. 42:119–129.
- Chin K-J, Lueders T, Friedrich MW, Klose M, Conrad R. 2004. Archaeal community structure and pathway of methane formation on rice roots. *Microb Ecol*. 47:59–67.
- Conrad R. 2005. Quantification of methanogenic pathways using stable carbon isotopic signatures: a review and a proposal. *Org Geochem*. 36:739–752.
- Conrad R, Chan O-C, Claus P, Casper P. 2007. Characterization of methanogenic Archaea and stable isotope fractionation during methane production in the profundal sediment of an oligotrophic lake (Lake Stechlin, Germany). *Limnol Oceanogr*. 52:1393–1406.
- Conrad R, Claus P, Casper P. 2009. Characterization of stable isotope fractionation during methane production in the sediment of a eutrophic lake, Lake Dagow, Germany. *Limnol Oceanogr*. 54:457–471.
- Conrad R, Erkel C, Liesack W. 2006. Rice Cluster I methanogens, an important group of Archaea producing greenhouse gas in soil. *Curr Opin Biotechnol*. 17:262–267.
- Costello AM, Lidstrom ME. 1999. Molecular characterization of functional and phylogenetic genes from natural populations of methanotrophs in lake sediments. *Appl Environ Microbiol*. 65:5066–5074.
- Daebeler A, Gansen M, Frenzel P. 2013. Methyl fluoride affects methanogenesis rather than community composition of methanogenic archaea in a rice field soil. *PLoS ONE*. 8.
- Davidson TA, Audet J, Jeppesen E, Landkildehus F, Lauridsen TL, S ondergaard M, Syv aranta J. 2018. Synergy between nutrients and warming enhances methane ebullition from experimental lakes. *Nat Clim Chang*. 8:156–160.
- Deutzmann JS, Schink B. 2011. Anaerobic oxidation of methane in sediments of Lake Constance, an oligotrophic freshwater lake. *Appl Environ Microbiol*. 77:4429–4436.
- Deutzmann JS, Stief P, Brandes J, Schink B. 2014. Anaerobic methane oxidation coupled to denitrification is the dominant methane sink in a deep lake. *P Nat Acad Sci USA*. 111:18273–18278.
- Duc NT, Crill P, Bastviken D. 2010. Implications of temperature and sediment characteristics on methane formation and oxidation in lake sediments. *Biogeochemistry*. 100:185–196.
- Earl J, Hall G, Pickup RW, Ritchie DA, Edwards C. 2003. Analysis of methanogen diversity in a hypereutrophic lake using PCR-RFLP analysis of *mcr* sequences. *Microb Ecol*. 46:270–278.
- Edgar RC, Haas BJ, Clemente JC, Quince C, Knight R. 2011. UCHIME improves sensitivity and speed of chimera detection. *Bioinforma*. 27:2194–2200.
- Erkel C, Kemnitz D, Kube M, Ricke P, Chin K-J, Dedysh S, Reinhardt R, Conrad R, Liesack W. 2005. Retrieval of first genome data for rice cluster I methanogens by a combination of cultivation and molecular techniques. *FEMS Microbiol Ecol*. 53:187–204.
- Escudero-Onate C. 2016. International cooperative programme on assessment and monitoring of acidification of rivers and lakes. Intercomparison 1630:pH, conductivity, alkalinity, NO₃-N, Cl, SO₄, Ca, Mg, Na, K, TOC, Al, Fe, Mn, Cd, Pb, Cu, Ni and Zn. Oslo, Norway: NIVA.
- Escudi e F, Auer L, Bernard M, Mariadassou M, Cauquil L, Vidal K, Maman S, Hernandez-Raquet G, Combes S, Pascal G. 2018. FROGS: find, rapidly, OTUs with Galaxy solution. *Bioinformatics*. 34:1287–1294.
- Ettwig KF, Butler MK, Le Paslier D, Pelletier E, Mangenot S, Kuypers MMM, Schreiber F, Dutilh BE, Zedelius J, de Beer D, et al. 2010. Nitrite-driven anaerobic methane oxidation by oxygenic bacteria. *Nature*. 464:543–548.
- Fuchs A, Lyautey E, Montuelle B, Casper P. 2016. Effects of increasing temperatures on methane concentrations and methanogenesis during experimental incubation of sediments from oligotrophic and mesotrophic lakes. *J Geophys Res G Biogeosciences*. 121:1394–1406.
- Galand PE, Saarnio S, Fritze H, Yrj al a K. 2002. Depth related diversity of methanogen Archaea in Finnish oligotrophic fen. *FEMS Microbiol Ecol*. 42:441–449.
- Hallam SJ, Girguis PR, Preston CM, Richardson PM, DeLong EF. 2003. Identification of methyl coenzyme M reductase A (*mcrA*) genes associated with methane-oxidizing archaea. *Appl Environ Microbiol*. 69:5483–5491.
- Hammer  , Harper D, Ryan P. 2001. PAST: Paleontological statistics software package for education and data analysis. *Palaeontol Electron*. 4:9.
- Happell JD, Chanton JP, Showers WS. 1994. The influence of methane oxidation on the stable isotopic composition of methane emitted from Florida swamp forests. *Geochim Cosmochim Acta*. 58:4377–4388.

- Haroon MF, Hu S, Shi Y, Imelfort M, Keller J, Hugenholtz P, Yuan Z, Tyson GW. 2013. Anaerobic oxidation of methane coupled to nitrate reduction in a novel archaeal lineage. *Nature*. 500:567–570.
- He R, Wooller MJ, Pohlman JW, Quensen J, Tiedje JM, Leigh MB. 2012. Shifts in identity and activity of methanotrophs in Arctic Lake sediments in response to temperature changes. *Appl Environ Microbiol*. 78:4715–4723.
- Holler T, Wegener G, Knittel K, Boetius A, Brunner B, Kuypers MMM, Widdel F. 2009. Substantial (13)C/(12)C and D/H fractionation during anaerobic oxidation of methane by marine consortia enriched in vitro. *Environ Microbiol Rep*. 1:370–376.
- Iino T, Mori K, Suzuki K-I. 2010. *Methanospirillum lacunae* sp. nov., a methane-producing archaeon isolated from a puddly soil, and emended descriptions of the genus *Methanospirillum* and *Methanospirillum hungatei*. *Int J Syst Evol Microbiol*. 60:2563–2566.
- Imachi H, Sakai S, Sekiguchi Y, Hanada S, Kamagata Y, Ohashi A, Harada H. 2008. *Methanolinea tarda* gen. nov., sp. nov., a methane-producing archaeon isolated from a methanogenic digester sludge. *Int J Syst Evol Microbiol*. 58:294–301.
- Iversen N, Jorgensen BB. 1993. Diffusion coefficients of sulfate and methane in marine sediment: influence of porosity. *Geochim Cosmochim Acta*. 57:571–578.
- Jetten MSM, Stams AJM, Zehnder AJB. 1992. Methanogenesis from acetate: a comparison of the acetate metabolism in *Methanotheroxobacter* and *Methanosarcina* spp. *FEMS Microbiol Lett*. 88:181–197.
- Johnson M, Zaretskaya I, Raytselis Y, Merezukh Y, McGinnis S, Madden TL. 2008. NCBI BLAST: a better web interface. *Nucleic Acids Res*. 36:W5–W9.
- Junier P, Junier T, Witzel KP. 2008. TRiFLe, a program for in silico terminal restriction fragment length polymorphism analysis with user-defined sequence sets. *Appl Environ Microbiol*. 74:6452–6456.
- Juottonen H, Galand PE, Yrjälä K. 2006. Detection of methanogenic Archaea in peat: comparison of PCR primers targeting the *mcrA* gene. *Res Microbiol*. 157:914–921.
- Kalinkina NM, Belkina NA, Polyakova TN, Syarki MT. 2013. Bioindication of the state of deep-water areas in Petrozavodsk Bay, Lake Onega, by macrozoobenthos characteristics. *Water Resour*. 40:528–534.
- Kojima H, Tsutsumi M, Ishikawa K, Iwata T, Mußmann M, Fukui M. 2012. Distribution of putative denitrifying methane oxidizing bacteria in sediment of a freshwater lake, Lake Biwa. *Syst Appl Microbiol*. 35:233–238.
- Kozich JJ, Westcott SL, Baxter NT, Highlander SK, Schloss PD. 2013. Development of a dual-index sequencing strategy and curation pipeline for analyzing amplicon sequence data on the miseq illumina sequencing platform. *Appl Environ Microbiol*. 79:5112–5120.
- Kulikova TP, Syarki MT. 2004. Effect of anthropogenic eutrophication on zooplankton distribution in Kondopoga Bay of Lake Onega. *Water Resour*. 31:85–91.
- Kumar S, Stecher G, Tamura K. 2016. MEGA7: Molecular evolutionary genetics analysis version 7.0 for bigger datasets, brief communication. *Mol Biol Evol*. 33:1870–1874.
- Liptay K, Chanton J, Czepiel P, Mosher B. 1998. Use of stable isotopes to determine methane oxidation in landfill cover soils. *J Geophys Res Atmos*. 103:8243–8250.
- Lloyd KG, Alperin MJ, Teske A. 2011. Environmental evidence for net methane production and oxidation in putative ANaerobic MEthanotrophic (ANME) archaea. *Environ Microbiol*. 13:2548–2564.
- Lueders T, Chin K-J, Conrad R, Friedrich M. 2001. Molecular analyses of methyl-coenzyme M reductase α -subunit (*mcrA*) genes in rice field soil and enrichment cultures reveal the methanogenic phenotype of a novel archaeal lineage. *Environ Microbiol*. 3:194–204.
- Lueders T, Friedrich MW. 2003. Evaluation of PCR amplification bias by terminal restriction fragment length polymorphism analysis of small-s rRNA and *mcrA* genes by using defined template mixtures of methanogenic pure cultures and soil DNA extracts. *Appl Environ Microbiol*. 69:320–326.
- Luesken FA, Zhu B, van Alen TA, Butler MK, Diaz MR, Song B, Op den Camp HJM, Jetten MSM, Ettwig KF. 2011. *pmoA* primers for detection of anaerobic methanotrophs. *Appl Environ Microbiol*. 77:3877–3880.
- Luton PE, Wayne JM, Sharp RJ, Riley PW. 2002. The *mcrA* gene as an alternative to 16S rRNA in the phylogenetic analysis of methanogen populations in landfill. *Microbiology*. 148:3521–3530.
- Maerki M, Wehrli B, Dinkel C, Müller B. 2004. The influence of tortuosity on molecular diffusion in freshwater sediments of high porosity. *Geochim Cosmochim Acta*. 68:1519–1528.
- Magoč T, Salzberg SL. 2011. FLASH: fast length adjustment of short reads to improve genome assemblies. *Bioinformatics*. 27:2957–2963.
- Mahé F, Rognes T, Quince C, de Vargas C, Dunthorn M. 2015. Swarm v2: highly-scalable and high-resolution amplicon clustering. *PeerJ*. 3:e1420.
- Meyers P. 1994. Preservation of elemental and isotopic source identification of sedimentary organic matter. *Chem Geol Isot Geosci Sect*. 114:289–302.
- Mori K, Harayama S. 2011. *Methanobacterium petrolearium* sp. nov. and *Methanobacterium ferruginis* sp. nov., mesophilic methanogens isolated from salty environments. *Int J Syst Evol Microbiol*. 61:138–143.
- Mori K, Iino T, Suzuki K-I, Yamaguchi K, Kamagata Y. 2012. Aceticlastic and NaCl-requiring methanogen “*Methanosaeta pelagica*” sp. nov., isolated from marine tidal flat sediment. *Appl Environ Microbiol*. AEM-07484.
- Nordi KA, Thamdrup B, Schubert CJ. 2013. Anaerobic oxidation of methane in an iron-rich Danish freshwater lake sediment. *Limnol Oceanogr*. 58:546–554.
- Nunoura T, Oida H, Miyazaki J, Miyashita A, Imachi H, Takai K. 2008. Quantification of *mcrA* by fluorescent PCR in methanogenic and methanotrophic microbial communities. *FEMS Microbiol Ecol*. 64:240–247.
- Oksanen J, Kindt R, Legendre P, O’Hara B, Stevens MHH, Oksanen MJ, Suggests M. 2007. The vegan package. *Community Ecol Packag*. 10.
- Oswald K, Milucka J, Brand A, Hach P, Littmann S, Wehrli B, Kuypers MMM, Schubert CJ. 2016. Aerobic gamma-proteobacterial methanotrophs mitigate methane emissions from oxic and anoxic lake waters. *Limnol Oceanogr*. 61:S101–S118.
- Pachauri RK, Allen MR, Barros VR, Broome J, Cramer W, Christ R, Church JA, Clarke L, Dahe Q, Dasgupta P. 2014. Climate change 2014: synthesis report. Contribution of Working Groups I, II and III to the fifth assessment report of the Intergovernmental Panel on Climate Change. IPCC.

- Palmer MA, Reidy Liermann CA, Nilsson C, Flörke M, Alcamo J, Lake PS, Bond N. 2008. Climate change and the world's river basins: anticipating management options. *Front Ecol Environ.* 6:81–89.
- Parkes RJ, Webster G, Cragg BA, Weightman AJ, Newberry CJ, Ferdelman TG, Kallmeyer J, Jørgensen BB, Aiello IW, Fry JC. 2005. Deep sub-seafloor prokaryotes stimulated at interfaces over geological time. *Nature.* 436:390–394.
- Quast C, Pruesse E, Yilmaz P, Gerken J, Schweer T, Yarza P, Peplies J, Glöckner FO. 2013. The SILVA ribosomal RNA gene database project: improved data processing and web-based tools. *Nucleic Acids Res.* 41:590–596.
- R Core Team. 2015. A language and environment for statistical. R Foundation for Statistical Computing, Vienna (Austria).
- Ramette A. 2009. Quantitative community fingerprinting methods for estimating the abundance of operational taxonomic units in natural microbial communities. *Appl Environ Microbiol.* 75:2495–2505.
- Randlett M-E, Sollberger S, Del Sontro T, Müller B, Corella JP, Wehrli B, Schubert CJ. 2015. Mineralization pathways of organic matter deposited in a river–lake transition of the Rhone River Delta, Lake Geneva. *Environ Sci Process Impacts.* 17:370–380.
- Rognes T, Flouri T, Nichols B, Quince C, Mahé F. 2016. VSEARCH: a versatile open source tool for metagenomics. *PeerJ.* 4:e2584.
- Roland FAE, Darchambeau F, Morana C, Bouillon S, Borges AV. 2016. Emission and oxidation of methane in a meromictic, eutrophic and temperate lake (Dendre, Belgium). *Chemosphere.* 168:756–764.
- Roussel EG, Sauvadet A-L, Allard J, Chaduteau C, Richard P, Bonavita M-AC, Chaumillon E. 2009. Archaeal methane cycling communities associated with gassy subsurface sediments of Marennes-Oléron Bay (France). *Geomicrobiol J.* 26:31–43.
- Sabylina AV, Lozovik PA, Zobkov MB. 2010. Water chemistry in Onega Lake and its tributaries. *Water Resour.* 37:842–853.
- Saitou N, Nei M. 1987. The neighbor-joining method: a new method for reconstructing phylogenetic trees. *Mol Biol Evol.* 4:406–425.
- Sakai S, Conrad R, Liesack W, Imachi H. 2010. *Methanocella arvoryzae* sp. nov., a hydrogenotrophic methanogen isolated from rice field soil. *Int J Syst Evol Microbiol.* 60:2918–2923.
- Sakai S, Ehara M, Tseng I-C, Yamaguchi T, Brauer SL, Cadillo-Quiroz H, Zinder SH, Imachi H. 2012. *Methanolinea mesophila* sp. nov., a hydrogenotrophic methanogen isolated from rice field soil, and proposal of the archaeal family Methanoregulaceae fam. nov. within the order Methanomicrobiales. *Int J Syst Evol Microbiol.* 62:1389–1395.
- Sakai S, Imachi H, Hanada S, Ohashi A, Harada H, Kamagata Y. 2008. *Methanocella paludicola* gen. nov., sp. nov., a methane-producing archaeon, the first isolate of the lineage “Rice Cluster I”, and proposal of the new archaeal order Methanocellales ord. nov. *Int J Syst Evol Microbiol.* 58:929–936.
- Sakai S, Imachi H, Sekiguchi Y, Tseng IC, Ohashi A, Harada H, Kamagata Y. 2009. Cultivation of methanogens under low-hydrogen conditions by using the coculture method. *Appl Environ Microbiol.* 75:4892–4896.
- Sansone FJ, Popp BN, Rust TM. 1997. Stable carbon isotopic analysis of low-level methane in water and gas. *Anal Chem.* 69:40–44.
- Sauniois M, Bousquet P, Poulter B, Pregon A, Ciais P, Canadell JG, Dlugokencky EJ, Etiope G, Bastviken D, Houweling S, et al. 2016. The global methane budget 2000–2012. *Earth Syst Sci Data.* 8:697–751.
- Schiff SL, Aravena R, Trumbore SE, Dillon PJ. 1990. Dissolved organic carbon cycling in forested watersheds: a carbon isotope approach. *Water Resour Res.* 26:2949–2957.
- Schloss PD, Westcott SL, Ryabin T, Hall JR, Hartmann M, Hollister EB, Lesniewski RA, Oakley BB, Parks DH, Robinson CJ, et al. 2009. Introducing mothur: open-source, platform-independent, community-supported software for describing and comparing microbial communities. *Appl Environ Microbiol.* 75:7537–7541.
- Schubert CJ, Vazquez F, Lösekann-Behrens T, Knittel K, Tonolla M, Boetius A. 2011. Evidence for anaerobic oxidation of methane in sediments of a freshwater system (Lago di Cadagno). *FEMS Microbiol Ecol.* 76:26–38.
- Schulz S, Conrad R. 1996. Influence of temperature on pathways to methane production in the permanently cold profundal sediment of Lake Constance. *FEMS Microbiol Ecol.* 20:1–14.
- Simankova M V, Kotsyurbenko OR, Lueders T, Nozhevnikova AN, Wagner B, Conrad R, Friedrich MW. 2003. Isolation and characterization of new strains of methanogens from cold terrestrial habitats. *Syst Appl Microbiol.* 26:312–318.
- Sivan O, Adler M, Pearson A, Gelman F, Bar-Or I, John SG, Eckert W. 2011. Geochemical evidence for iron-mediated anaerobic oxidation of methane. *Limnol Oceanogr.* 56:1536–1544.
- Slesarev AI, Mezhevaya K V, Makarova KS, Polushin NN, Shcherbinina O V, Shakhova V V, Belova GI, Aravind L, Natale DA, Rogozin IB. 2002. The complete genome of hyperthermophile *Methanopyrus kandleri* AV19 and monophyly of archaeal methanogens. *P Nat Acad Sci USA.* 99:4644–4649.
- Sollberger S, Corella JP, Girardclos S, Randlett ME, Schubert CJ, Senn DB, Wehrli B, DelSontro T. 2014. Spatial heterogeneity of benthic methane dynamics in the subaquatic canyons of the Rhone River Delta (Lake Geneva). *Aquat Sci.* 76:89–101.
- Springer E, Sachs MS, Woese CR, Boone DR. 1995. Partial gene sequences for the A subunit of methyl-coenzyme M reductase (mcrI) as a phylogenetic tool for the family Methanosarcinaceae. *Int J Syst Evol Microbiol.* 45:554–559.
- Steinberg LM, Regan JM. 2008. Phylogenetic comparison of the methanogenic communities from an acidic, oligotrophic fen and an anaerobic digester treating municipal wastewater sludge. *Appl Environ Microbiol.* 74:6663–6671.
- Steinberg LM, Regan JM. 2009. mcrA-targeted real-time quantitative PCR method to examine methanogen communities. *Appl Environ Microbiol.* 75:4435–4442.
- Sundh I, Bastviken D, Tranvik LJ. 2005. Abundance, activity, and community structure of pelagic methane-oxidizing bacteria in temperate lakes. *Appl Environ Microbiol.* 71:6746–6752.
- Svenning MM, Hestnes AG, Wartianen I, Stein LY, Klotz MG, Kalyuzhnaya MG, Spang A, Bringel F, Vuilleumier S, Lajus A, et al. 2011. Genome sequence of the Arctic methanotroph

- Methylobacter tundripaludum* SV96. J Bacteriol. 193:6418–6419.
- Tekanova EV. 2012. The contribution of primary production to organic carbon content in Lake Onego. Inl Water Biol. 5:328–332.
- Tyler SC, Bilek RS, Sass RL, Fisher FM. 1997. Methane oxidation and pathways of production in a Texas paddy field deduced from measurements of flux, $\delta^{13}\text{C}$, and δD of CH_4 . Glob Biogeochem Cy. 11:323–348.
- Wang Y, Qian PY. 2009. Conservative fragments in bacterial 16S rRNA genes and primer design for 16S ribosomal DNA amplicons in metagenomic studies. PLoS ONE. 4:e7401
- Wartiainen I, Hestnes AG, McDonald IR, Svenning MM. 2006. *Methylocystis rosea* sp. nov., a novel methanotrophic bacterium from Arctic wetland soil, Svalbard, Norway (78° N). Int J Syst Evol Microbiol. 56:541–547.
- Watanabe T, Kimura M, Asakawa S. 2009. Distinct members of a stable methanogenic archaeal community transcribe mcrA genes under flooded and drained conditions in Japanese paddy field soil. Soil Biol Biochem. 41:276–285.
- Welte CU, Rasigraf O, Vaksmaa A, Versantvoort W, Arshad A, Op Den Camp HJM, Jetten MSM, Lüke C, Reimann J. 2016. Nitrate- and nitrite-dependent anaerobic oxidation of methane. Environ Microbiol Rep. 8:941–955.
- Wersin P, Höhener P, Giovanoli R, Stumm W. 1991. Early diagenetic influences on iron transformations in a freshwater lake sediment. Chem Geol. 90:233–252.
- West WE, Creamer KP, Jones SE. 2016. Productivity and depth regulate lake contributions to atmospheric methane. Limnol Oceanogr. 61:S51–S61.
- Whiticar MJ. 1999. Carbon and hydrogen isotope systematics of bacterial formation and oxidation of methane. Chem Geol. 161:291–314.
- Whiticar MJ, Faber E. 1986. Methane oxidation in sediment and water column environments – isotope evidence. Org Geochem. 10:759–768.
- Yashiro Y, Sakai S, Ehara M, Miyazaki M, Yamaguchi T, Imachi H. 2011. *Methanoregula formicica* sp. nov., a methane-producing archaeon isolated from methanogenic sludge. Int J Syst Evol Microbiol. 61:53–59.
- Zobkov MB, Zobkova MV. 2015. A device for determination of organic carbon in water with photochemical persulfate oxidation in the system of continuous gas flow and FTIR spectrometric detection. Fact Lab Diagnostics Mater. 81:10–15.